

1 **Title: A high resolution atlas of gene expression in the domestic**
2 **sheep (*Ovis aries*)**

3

4 Clark EL^{1*}, Bush SJ^{1∅}, McCulloch MEB¹, Farquhar IL^{1‡}, Young R¹, Lefevre L¹,
5 Pridans C¹, Tsang HG¹, Watson M¹, Whitelaw CB¹, Freeman TC¹, Summers KM¹,
6 Archibald AL¹ and Hume DA¹

7

8 ¹The Roslin Institute and Royal (Dick) School of Veterinary Studies, University of
9 Edinburgh, Easter Bush Campus, Edinburgh, Midlothian, EH25 9RG.

10 [‡]Current Address: Centre for Synthetic and Systems Biology, CH Waddington
11 Building, Max Borne Crescent, Kings Buildings, University of Edinburgh, EH9 3BF.

12 [∅] These two authors contributed equally to the work.

13 * Corresponding Author: emily.clark@roslin.ed.ac.uk

14

15

16

17

18

19

20

21

22

23

24

25

26 **Abstract**

27

28 Sheep are a key source of meat, milk and fibre for the global livestock sector, and an
29 important biomedical model. Global analysis of gene expression across multiple
30 tissues has aided genome annotation and supported functional annotation of
31 mammalian genes. We present a large-scale RNA-Seq dataset representing all the
32 major organ systems from adult sheep and from several juvenile, neonatal and
33 prenatal developmental time points. The *Ovis aries* reference genome (Oar v3.1)
34 includes 27,504 genes (20,921 protein coding), of which 25,350 (19,921 protein
35 coding) had detectable expression in at least one tissue in the sheep gene
36 expression atlas dataset. Network-based cluster analysis of this dataset grouped
37 genes according to their expression pattern. The principle of ‘guilt by association’
38 was used to infer the function of uncharacterised genes from their co-expression
39 with genes of known function. We describe the overall transcriptional signatures
40 present in the sheep gene expression atlas and assign those signatures, where
41 possible, to specific cell populations or pathways. The findings are related to innate
42 immunity by focusing on clusters with an immune signature, and to the advantages
43 of cross-breeding by examining the patterns of genes exhibiting the greatest
44 expression differences between purebred and crossbred animals. This high-
45 resolution gene expression atlas for sheep is, to our knowledge, the largest
46 transcriptomic dataset from any livestock species to date. It provides a resource to
47 improve the annotation of the current reference genome for sheep, presenting a
48 model transcriptome for ruminants and insight into gene, cell and tissue function at
49 multiple developmental stages.

50

51

52 **Abbreviations**

53 AM, Alveolar Macrophage; BFxT, Scottish Blackface x Texel; BMDM, Bone Marrow
54 Derived Macrophage; CNS, Central Nervous System; DE, Differential Expression;
55 EBI, European Bioinformatics Institute; ENA, European Nucleotide Archive; FAANG,
56 Functional Annotation of ANimal Genomes; GI, Gastrointestinal; HGNC, HUGO
57 (Human Genome Organisation) Gene Nomenclature Committee; LPS,
58 Lipopolysaccharide; MCL, Markov Cluster Algorithm; MCLi, Markov Cluster
59 Algorithm Inflation; MDM, Monocyte Derived Macrophage; mRNA, messenger
60 Ribonucleic Acid; NF- κ B, Nuclear Factor Kappa-Light-Chain-Enhancer of Activated
61 B-Cells; PBMC, Peripheral Blood Mononuclear Cell; RNA-Seq, RNA Sequencing;
62 PPAR, Peroxisome Proliferator-Activated Receptor; rhCSF1, Recombinant Human
63 Colony Stimulating Factor 1; SIGLEC, Sialic Acid-Binding Immunoglobulin-Like
64 Lectin; SNP, Single Nucleotide Polymorphism

65

66 **Background**

67 Sheep (*Ovis aries*) represent an important livestock species globally and are
68 a key source of animal products including meat, milk and fibre. They remain an
69 essential part of the rural economy in many developed countries and are central to
70 sustainable agriculture in developing countries. They are also an important source
71 of greenhouse gases [1]. Although genetic improvement is often considered to have
72 been less effective in sheep than in the dairy cattle, pig and poultry sectors,
73 advanced genomics-enabled breeding schemes are being implemented in New
74 Zealand and elsewhere [2-4]. A better understanding of functional sequences,
75 including transcribed sequences and the transcriptional control of complex traits

76 such as disease resilience, reproductive capacity, feed conversion efficiency and
77 welfare, will enable further improvements in productivity with concomitant reductions
78 in environmental impact.

79 RNA-Sequencing (RNA-Seq) has transformed the analysis of gene
80 expression from the single-gene to the genome-wide scale allowing visualisation of
81 the transcriptome and re-defining how we view the transcriptional control of complex
82 traits (reviewed in [5]). Large-scale gene expression atlas projects have defined the
83 mammalian transcriptome in multiple species, initially using microarrays [6-9] and
84 more recently by the sequencing of full length transcripts or of 5' ends by the
85 FANTOM 5 consortium [10-12], ENCODE project [13] and Genotype-Tissue
86 Expression (GTEx) Consortium [14].

87 These efforts have focused mainly on mice and humans, for which there are
88 high quality richly annotated reference genome sequences available as a frame of
89 reference for the identification and analysis of transcribed sequences. Draft
90 reference genome sequences have been established for the major livestock species
91 (chicken, pig, sheep, goat and cattle) over the past decade, yet it is only with the
92 recent deployment of long read sequencing technology that the contiguity of the
93 reference genome sequences for these species has improved. This is exemplified by
94 the recent goat genome assembly [15, 16]. In these species there are still many
95 predicted protein-coding and non-coding genes for which the gene model is incorrect
96 or incomplete, or where there is no informative functional annotation. For example, in
97 the current sheep reference genome, Oar v3.1 (Ensembl release 87)
98 (http://www.ensembl.org/Ovis_aries/Info/Index), 30% of protein-coding genes are
99 identified with an Ensembl placeholder ID [17]. Given the high proportion of such
100 unannotated genes many are likely to be involved in important functions. Large-

101 scale RNA-Seq gene expression datasets can be utilised to understand the
102 underlying biology and annotate and assign function to such unannotated genes
103 [18]. With sufficiently large datasets, genes form co-expression clusters, which can
104 either be generic, associated with a given pathway or be cell-/tissue- specific. This
105 information can then be used to associate a function with genes co-expressed in the
106 same cluster, a logic known as the 'guilt by association principle' [19]. Detailed
107 knowledge of the expression pattern can provide a valuable window on likely gene
108 function, as demonstrated in pig [6], sheep [17, 20], human and mouse [8, 9, 21, 22].

109 A high quality well-annotated reference genome is an exceptionally valuable
110 resource for any livestock species, providing a comparative sequence dataset and a
111 representative set of gene models. The International Sheep Genomics Consortium
112 (ISGC) released a high quality draft sheep genome sequence (Oar v3.1) in 2014
113 [17]. Included in the sheep genome paper were 83 RNA-Seq libraries from a Texel
114 gestating adult female, 16 day embryo, 8 month old lamb and an adult ram. This
115 Texel RNA-Seq transcriptome significantly improved the annotation of Oar v3.1 and
116 identified numerous genes exhibiting changes in copy number and tissue specific
117 expression [17]. To build on this resource and further improve the functional
118 annotation of Oar v3.1 we have generated a much larger high-resolution
119 transcriptional atlas from a comprehensive set of tissues and cell types from multiple
120 individuals of an outbred cross of two economically important sheep breeds. To
121 maximize heterozygosity we deliberately chose a cross of disparate breeds, the
122 Texel, which is used as a terminal sire as it is highly muscled in some cases
123 because it has a myostatin variant linked to double-muscling and meat quality [23],
124 and the Scottish Blackface, a breed selected for robustness on marginal upland
125 grazing [24].

126 The sheep gene expression atlas dataset presented here is the largest of its
127 kind from any livestock species to date and includes RNA-Seq libraries from tissues
128 and cells representing all the major organ systems from adult sheep and from
129 several juvenile, neonatal and prenatal developmental time points. Because the
130 tissues were obtained from multiple healthy young adult animals, the atlas may also
131 aid understanding of the function of orthologous human genes. Our aim was to
132 provide a model transcriptome for ruminants and give insight into gene, cell and
133 tissue function and the molecular basis of complex traits. To illustrate the value of
134 the resource, we provide detailed examination of genes implicated in innate
135 immunity and the advantages of cross breeding and provide putative gene names for
136 hundreds of the unannotated genes in Oar v3.1. The entire data set is available in a
137 number of formats to support the research community and will contribute to the
138 Functional Annotation of Animal Genomes (FAANG) project [25, 26].

139

140 **Results and Discussion**

141 **Scope of Sheep Gene Expression Atlas Dataset**

142 This sheep gene expression atlas dataset expands on the RNA-Seq datasets
143 already available for sheep, merging a new set of 429 RNA-Seq libraries from the
144 Scottish Blackface x Texel cross (BFxT) with 83 existing libraries from Texel [17].
145 Details of the new BFxT libraries generated for the sheep gene expression atlas,
146 including the developmental stages sampled, tissue/cell types and sex of the
147 animals are summarised in Table 1. These samples can be grouped into 4 subsets
148 (“Core Atlas”, “GI Tract Time Series”, “Early Development” and “Maternal
149 Reproductive Time Series”). The animals used to generate the four subsets of
150 samples are detailed in S1 Table.

151 The “Core Atlas” subset was generated using six adult virgin sheep,
152 approximately 2 years of age. Tissue samples were collected from all major organ
153 systems from 3 males and 3 females to ensure, wherever possible, there were
154 biological replicates from each sex to support an analysis of sex-specific gene
155 expression. In addition, five cell types were sampled, including peripheral blood
156 mononuclear cells (PBMCs) and blood leukocytes. Since macrophages are known
157 to be a highly complex source of novel mRNAs [27], and were not sampled
158 previously, three types of macrophage (+/- stimulation with lipopolysaccharide (LPS))
159 were included.

160 For the “GI Tract Time Series” subset of samples we focused on 10 regions of
161 the gastro-intestinal (GI) tract, immediately at birth prior to first feed, at one week
162 and at 8 weeks of age. These time points aimed to capture the transition from milk-
163 feeding to rumination. Embryonic time points were chosen, at days 23, 35 and 100,
164 to detect transcription in the liver, ovary and brain in “Early Development”. Parallel
165 time points were included for placenta and ovary samples from gestating BFXT
166 ewes, comprising the “Maternal Reproductive Time Series” subset. Finally, 3 pools
167 of eight day 7 blastocysts were included to measure transcription pre-implantation
168 and these were also included in the “Early Development” subset.

169 A detailed list of all tissues and cell types included in each subset of samples
170 can be found in S2 Table. Tissues and cell types were chosen to give as
171 comprehensive a set of organ systems as possible and include those tissues
172 relevant for phenotypic traits such as muscle growth and innate immunity.

173

174 **Sequencing Depth and Coverage**

175 Approximately 37×10^9 sequenced reads were generated from the BFXT
176 libraries, generating approximately 26×10^9 alignments in total. The raw number of
177 reads and percentage of alignable reads per sample are included in S3 Table. For
178 each tissue a set of expression estimates, as transcripts per million (TPM), were
179 obtained using the high speed transcript quantification tool Kallisto [28]. Kallisto is a
180 new transcriptome-based quantification tool that avoids the considerable bias
181 introduced by the genome alignment step [29]. Gene level expression atlases are
182 available as S1 Supplementary File and, with expression estimates averaged per
183 tissue per developmental stage, S2 Supplementary File. The data were corrected for
184 library type (as we described in [30] and summarised in S3 Supplementary File). We
185 used Principal Component Analysis (PCA) pre- and post-correction (S1 Fig) for
186 library type to ensure the correction was satisfactory. Hierarchical clustering of the
187 samples is included in (Fig 1) and illustrates both the large diversity and logical
188 clustering of samples of samples included in the dataset.

189 The *O. aries* reference genome (Oar v3.1) includes 27,504 loci that are
190 transcribed (20,921 protein coding), of which 25,350 (19,921 protein coding) (97%)
191 were detectable with expression of TPM >1, in at least one tissue from at least one
192 individual, in the sheep gene expression atlas dataset, demonstrating the depth and
193 scope of this dataset. The proportion of transcripts with detectable expression, after
194 each 'pass' with Kallisto (See Materials and Methods), is presented in Table 2. Only
195 3% (561) of transcripts from Oar v3.1 (S4 Table) did not meet the minimum detection
196 threshold of TPM > 1 in at least one tissue and therefore were not detected in the
197 sheep atlas dataset. In a minority of cases, transcripts were missing because they
198 were highly specific to a tissue or cell which was not sampled, such as odontoblasts
199 (which uniquely produce tooth dentin, mediated by DSPP (dentin

200 sialophosphoprotein) [33]). We also did not include any samples taken from the eye
201 which expresses multiple unique proteins e.g., the lens-specific enzyme LGSN
202 (lengsin) [34]. The majority (77%) of the genes not detected in the sheep atlas were
203 unannotated, with no assigned gene name. A small number of these genes (36) lack
204 sequence conservation and coding potential and so are potentially spurious models
205 (S4 Table).

206

207 **Gene Annotation**

208 In the Oar v3.1 annotation, 6217 (~30%) of the protein coding genes lack an
209 informative gene name. Whilst the Ensembl annotation will often identify
210 homologues of a sheep gene model, the automated annotation pipeline used is
211 conservative in its assignment of gene names and symbols. Using an annotation
212 pipeline (described in S3 Supplementary File and illustrated in S5 Table) we were
213 able to utilise the sheep gene expression atlas dataset to annotate >1000 of the
214 previously unannotated protein coding genes in Oar v3.1 (S6 Table). These genes
215 were annotated by reference to the NCBI non-redundant (nr) peptide database v77
216 [35] and assigned a quality category based on reciprocal percentage identity, if any,
217 to one of 9 known ruminant proteomes (S7 Table). A short-list containing a
218 conservative set of gene annotations, to HGNC (HUGO Gene Nomenclature
219 Committee) gene symbols, is included in S8 Table. Many of these genes are
220 found in syntenic regions, and are also supported by the up- and downstream
221 conservation of genes in a related genome, cattle (*Bos taurus* annotation UMD 3.1).
222 S9 Table contains the full list of genes annotated using this pipeline. Many
223 unannotated genes can be associated with a gene description, but not necessarily
224 an HGNC symbol; these are also listed in S10 Table. We manually validated the

225 assigned gene names on this longer list using network cluster analysis and the “guilt
226 by association” principle.

227

228 **Network Cluster Analysis**

229 Network cluster analysis of the sheep gene expression atlas was performed
230 using Miru (Kajeka Ltd, Edinburgh UK), a tool for the visualisation and analysis of
231 network graphs from big data [36-38]. The the atlas of unaveraged TPM estimates,
232 available as S1 Supplementary File, were used for the network cluster analysis. The
233 three blastocyst samples were removed from the network cluster analysis as they
234 were generated using a library preparation method which was not corrected for and
235 created a significant effect of library type. With a Pearson correlation co-efficient
236 threshold of $r=0.75$ and MCL (Markov Cluster Algorithm [39]) inflation value of 2.2,
237 the gene-to-gene network comprised 15,129 nodes (transcripts) and 811,213 edges
238 (correlations above the threshold value). This clustering excludes >30% of detected
239 transcripts, most of which had idiosyncratic expression profiles. One of the major
240 sources of unique expression patterns is the use of distinct promoters in different cell
241 types. The transcription factor *MITF* (Melanogenesis Associated Transcription
242 Factor), for example, does not cluster with any other transcripts in sheep and is
243 known in humans to have at least 7 distinct tissue-specific promoters in different cell
244 types, including macrophages, melanocytes, kidney, heart and retinal pigment
245 epithelium [12].

246 The resultant correlation network (Fig 2) was very large and highly structured
247 comprising of 309 clusters ranging in size. Genes found in each cluster are listed in
248 S11 Table and clusters 1 to 50 (numbered in order of size; cluster 1 being made up
249 of 1199 genes) were annotated by hand and assigned a broad functional ‘class’ and

250 'sub-class' (Table 3). Functional classes were assigned based on GO term
251 enrichment [40] for molecular function and biological process (S12 Table) and gene
252 expression pattern, as well as comparison with functional groupings observed in the
253 pig expression atlas [6]. Fig 3 shows a network graph with the nodes collapsed, and
254 the largest clusters numbered 1 to 30, to illustrate the relative number of genes in
255 each cluster and their functional class.

256 The majority of co-expression clusters included genes exhibiting a specific
257 cell/tissue expression pattern (Fig 4A). There were a few exceptions, including the
258 largest cluster (cluster 1), which contained ubiquitously expressed 'house-keeping'
259 genes, encoding proteins that are functional in all cell types. The high proportion of
260 unannotated genes (24% of the 1199 genes) in cluster 1 may reflect the focus of
261 functional genomics on genes exhibiting tissue specific expression, and inferred
262 function in differentiation, leaving those with a house-keeping function
263 uncharacterised [41]. With a few exceptions, the remaining co-expression clusters
264 were comprised of genes exhibiting either expression only in a distinct tissue or cell
265 type expression pattern e.g. macrophages (cluster 5) (Fig 4B (i)) and fetal ovary
266 (cluster 7) (Fig 4B (ii)), or a broader expression pattern associated with a cellular
267 process e.g. oxidative phosphorylation (cluster 15) (Fig 4B (iii)). Some co-expression
268 is shared between two or more organ systems, associated with known shared
269 functions. For example, cluster 15, exhibiting high expression in liver and kidney
270 cortex, is enriched for expression of genes relating to the oxidation-reduction
271 process, transmembrane transport, monocarboxylic acid catabolic process and fatty
272 acid oxidation (S13 Table). It includes numerous genes encoding enzymes involved
273 in amino acid catabolism (e.g. *AGXT*, *AGXT2*, *ASPDH*, *ACY1*, *EHHADH*, *DPYD*,
274 *DAO*, *DDO*, *HAO1*, and *HPD*) and the rate-limiting enzymes of gluconeogenesis

275 (*PCK1*, *PC*, *ALDOB* and *G6PC*). The contributions of kidney and liver to amino acid
276 turnover and gluconeogenesis are well known in humans [42] and rodents [43].
277 These observations suggest that the shared catabolic pathways of liver and kidney
278 cortex are largely conserved in sheep, but detailed curation of the genes in this
279 cluster could provide further specific insights. Alanine aminotransferase (*ALT1*
280 synonym *GPT1*), which generates alanine from the breakdown of amino acids in
281 muscle and is transported to the liver for gluconeogenesis, is highly-expressed in
282 muscle as expected. The glutaminase genes, required for the turnover of glutamine,
283 are absent from tissue or cell type specific clusters; the liver-specific enzyme *GLS2*
284 is also expressed in neuronal tissues, as it is in humans [44, 45].

285 The tissue-specific expression patterns observed across clusters showed a
286 high degree of similarity to those observed for pig [6], human and mouse [8, 9]. In
287 some cases we were able to add functional detail to clusters of genes previously
288 observed in pig and human. For example, genes within cluster 6 showed high
289 expression in the fallopian tube and to a lesser extent the testes. Significantly
290 enriched GO terms for cluster 6 included cilium ($p=4.1 \times 10^{-8}$), microtubule motor
291 activity ($p=2.9 \times 10^{-11}$) and motile cilium ($p=2.8 \times 10^{-19}$) suggesting the genes expressed
292 in cluster 6 are likely to have a function related to motile cilia in sperm cells and the
293 fallopian tube. Cluster 6 in the sheep atlas dataset corresponds to cluster 9 in the pig
294 gene expression atlas [6]. Similarly, significantly enriched GO terms for genes in
295 cluster 28 included primary cilium ($p=7.5 \times 10^{-21}$) and ciliary basal body ($p=1.9 \times 10^{-12}$),
296 indicating the genes in this cluster were associated with the function of primary cilia.
297 Genes within this cluster showed a relatively wide expression pattern, with brain and
298 reproductive tissues exhibiting the highest expression. For both clusters associated
299 with ciliary function, significantly enriched GO terms also included cell-cycle related

300 cellular processes and cell-cycle associated genes, supporting the link between cilia
301 and the cell-cycle [46-48].

302

303 **Cellular Processes**

304 The genes within some clusters, rather than being linked to the function of a
305 particular tissue or cell type, showed varying levels of expression across multiple
306 tissues, suggesting their involvement in a universal cellular process (pathway).
307 Significantly enriched GO terms for genes in cluster 8, for example, included 'cell
308 cycle checkpoint' ($p=1 \times 10^{-17}$) and 'mitotic cell cycle' ($p < 1 \times 10^{-30}$). The variation in
309 expression of these genes across tissues likely reflects variation in the proportion of
310 mitotically active cells. In the same way, it is possible to extract a similar cluster from
311 large cancer gene expression data sets, correlating with their proliferative index [49].
312 Expression of genes in cluster 15 ($n=182$) was detectable in most ovine tissues and
313 cells but with strongly-enriched expression in skeletal and cardiac muscle. The pig
314 gene expression atlas [6] highlighted an oxidative phosphorylation cluster and a
315 mitochondrial/tricarboxylic acid (TCA) cluster. This functional grouping is merged in
316 cluster 15. The majority of the transcripts in cluster 15 are present within the
317 inventory of mitochondrial genes in humans and mice [50], but the reciprocal is not
318 true since many other genes encoding proteins that locate to mitochondria were not
319 found in cluster 15. Many mitochondrial proteins are unrelated to oxidative
320 phosphorylation *per se*, and are enriched in other tissues including liver and kidney
321 (including mitochondrial enzymes of amino acid and fatty acid catabolism, see
322 above) and intestine.

323 Cluster 15 also contains several genes associated with myosin and the
324 sarcoplasmic reticulum which may indicate some level of coordination of their

325 function with the oxidative metabolism of glucose. The majority of genes in the
326 corresponding cluster in pig [6] were also present in this cluster with a few notable
327 additions including dihydrolipoamide dehydrogenase (*DLD*), which encodes a
328 member of the class-I pyridine nucleotide-disulfide oxidoreductase family, and
329 carnitine acetyltransferase (*CRAT*), a key enzyme in the metabolic pathway in
330 mitochondria [51]. We were able to assign gene names to the following genes
331 associated with oxidative phosphorylation complex I in pig: *NDUFA9*
332 (ENSOARG00000009435), *NDUFB1* (ENSOARG00000020197), *NUDFB8*
333 (assigned to ENSOARG00000015378), and *NDUFC2* (ENSOARG00000006694).
334 The gene name *PTGES2* (prostaglandin E2 synthase 2) was assigned to
335 ENSOARG00000010878, a gene that was associated with fatty acid (long-chain)
336 beta oxidation in pig [6] but previously unannotated in sheep. Similarly, we assigned
337 the gene name *PDHB* (pyruvate dehydrogenase E1 component subunit beta), a
338 member of the pyruvate dehydrogenase complex also previously unannotated in
339 sheep, to ENSOARG00000012222. The inclusion of the PDH complex, as well as
340 the mitochondrial pyruvate carriers *MPC1* and *MPC2*, in the muscle-enriched cluster
341 15 reflects the fact that glucose, giving rise to pyruvate, is the preferred fuel for
342 oxidative metabolism in muscle [52].

343 By using comparative clustering information in the pig and the “guilt by
344 association” principle we were able to assign with confidence gene names and
345 putative function to the majority of unannotated genes in clusters 8 (cell-cycle) and
346 15 (oxidative phosphorylation) (S13 Table). Expression of cell cycle and metabolic
347 genes has recently been shown to be positively correlated with dry matter intake,
348 ruminal short chain fatty acid concentrations and methane production in sheep [53].
349 In the same study a weak correlation between lipid/oxo-acid metabolism genes and

350 methane yield was also identified suggesting that the newly unannotated genes in
351 these clusters are likely to be relevant in addressing methane production in
352 ruminants [53].

353

354 **The GI Tract**

355 Stringent coexpression clustering requires that each transcript is quantified in
356 a sufficiently large number of different states to establish a strong correlation with all
357 other transcripts with which it shares coordinated transcription and, by implication, a
358 shared function or pathway. The impact of this approach was evident from the pig
359 gene expression atlas [6] which was effective at dissecting region-specific gene
360 expression in the GI tract. We have generated a comparable dataset for sheep. In
361 ruminants, the rumen, reticulum and omasum are covered exclusively with stratified
362 squamous epithelium similar to that observed in the tonsil [17, 20]. Each of these
363 organs has a very distinctive mucosal structure, which varies according to region
364 sampled [54]. A network cluster analysis of regions of the GI tract from sheep has
365 been published [20] using the Texel RNA-Seq dataset [17]. These co-expression
366 clusters are broken up somewhat in this larger atlas, because many of the genes
367 that are region-specific in the GI tract are also expressed elsewhere. We have, in
368 addition, expanded the available dataset for the GI tract to include samples from
369 neonatal and juvenile lambs.

370 The postnatal development of the sheep GI tract is of particular interest
371 because of the pre-ruminant to ruminant transition, which occurs over 8 weeks from
372 birth. Genes in cluster 33 showed low levels of expression in neonatal lambs and a
373 gradual increase into adulthood. Enriched GO terms for this cluster include
374 regulation of interleukin 6 (IL6) production ($p=0.0016$) and keratinocyte differentiation

375 ($p=1.7 \times 10^{-8}$) (S12 Table). The cluster includes genes such as *HMGCS2*, *HMGCL*
376 and *BDH1*, required for ketogenesis, an essential function of rumen metabolism, as
377 well as *CA1* (carbonic anhydrase 1), implicated in the rumen-specific uptake of short
378 chain fatty acids. The cluster does not contain any of the solute carriers implicated
379 in nutrient uptake in the rumen, suggesting that these are more widely-expressed
380 and/or regulated from multiple promoters [20]. The only carrier that is rumen-
381 enriched is *SLC9A3* (also known as *NHE3*), the key Na-H antiporter previously
382 implicated in rumen sodium transport in both sheep and cattle [55]. Other genes in
383 cluster 33, for example, *IL36A* and *IL36B*, for example, are thought to influence skin
384 inflammatory response by acting on keratinocytes and macrophages and indirectly
385 on T-lymphocytes to drive tissue infiltration, cell maturation and cell proliferation [56].
386 Many of these genes might also be part of the acute phase immune response, by
387 regulating production of key cytokines such as *IL-6* and thus mediating activation of
388 the NF- κ B signaling pathways. Nuclear factor (NF)- κ B and inhibitor of NF- κ B kinase
389 (IKK) proteins regulate innate- and adaptive-immune responses and inflammation
390 (reviewed in [57]). Expression of many of these genes is likely to change as the
391 immune system develops which we will describe in detail in a dedicated network
392 cluster analysis of the GI tract developmental time series dataset. The genes in this
393 cluster therefore appear to be involved both in the onset of rumination and in innate
394 immunity (which could be associated with the population of the rumen microbiome).

395

396 **Innate and Acquired Immunity**

397 Several clusters exhibited a strong immune signature. Clusters 11, 12, 18, 31
398 and 32, for example, contained genes with a strong T-lymphocyte signature [58] with
399 high levels of expression in immune cell types and lymphoid tissues. Significantly

400 enriched GO terms for cluster 12, for example, included T-cell differentiation
401 ($p=2.10 \times 10^{-11}$), immune response ($p=0.00182$) and regulation of T-cell activation
402 ($p=0.00019$) (S12 Table). Manual gene annotation using Ensembl IDs within this
403 cluster revealed the majority were T-cell receptors and T-cell surface glycoproteins
404 (S14 Table). Interestingly, ENSOARG00000008993 represents a gene with no
405 orthologues to other species within the Ensembl database, but partial blast hits to T-
406 lymphocyte surface antigen *Ly-9* in mouflon, goat, bison and buffalo in the NCBI
407 database. The 'true' gene LY9, a member of the signalling lymphocyte activation
408 molecule (SLAM) family [59], is also unannotated in sheep and is assigned to
409 ENSOARG00000008981, having multiple orthologues in other placental mammals.
410 We have assigned ENSOARG00000008993 the gene name 'LY9-like' and the
411 symbol *LY9L*, and suggest this transcript plays a role in T-lymphocyte pathogen
412 recognition.

413 Other immune clusters exhibited a macrophage-specific signature, with
414 subsets highly expressed in alveolar macrophages (AMs), monocyte derived
415 macrophages (MDMs) and bone marrow derived macrophages (BMDMs) (cluster 5)
416 and two defined clusters of genes induced in BMDMs stimulated with LPS (cluster
417 45 and 52). Known macrophage-specific surface markers, receptors and
418 proinflammatory cytokines predominated in these clusters, in addition to numerous
419 unannotated genes, with as yet undefined but probable immune function (S15
420 Table). For example, the *CD63* antigen, which mediates signal transduction events,
421 was assigned to ENSOARG00000011313 and *BST2* (bone marrow stromal cell
422 antigen 2), which is part of the interferon (IFN) alpha/beta signaling pathway, to
423 ENSOARG00000016787. A third cluster of LPS-inducible genes in macrophages,
424 cluster 64, contained a subset of the IFN-inducible antiviral effector genes, including

425 *DDX58*, *IFIT1*, *IFIT2*, *MX1*, *MX2*, *RSAD2* and *XAF1*, which are induced in mouse
426 and humans through the MyD88-independent *TLR4* signaling pathway via autocrine
427 *IFNB1* signaling (reviewed in [60]). Many other components of this pathway identified
428 in LPS-stimulated human macrophages [61] were either not annotated, or not
429 clustered, and will be the target of detailed annotation efforts in the macrophage
430 dataset.

431 Significantly enriched GO terms for the macrophage-specific cluster 5
432 included 'response to lipopolysaccharide' ($p=7.2 \times 10^{-7}$), and 'toll-like receptor
433 signaling pathway' ($p=3.2 \times 10^{-5}$). Many of the genes in this cluster are known
434 components of the innate immune response in mammals. Interleukin 27 (*IL-27*), is a
435 heterodimeric cytokine which has pro- and anti-inflammatory properties and a
436 diverse effect on immune cells including the regulation of T-helper cell development,
437 stimulation of cytotoxic T-cell activity and suppression of T-cell proliferation [62].
438 *ADGRE1* encodes the protein EGF-like module-containing mucin-like hormone
439 receptor-like 1 (*EMR1* also known as F4/80), a classic macrophage marker in mice
440 [63]. Several genes in cluster 5 encode proteins exclusively expressed in
441 macrophages and monocytes. One such gene, *CD163*, encodes a member of the
442 scavenger receptor cysteine-rich (SRCR) superfamily, which protects against
443 oxidative damage by the clearance and endocytosis of hemoglobin/haptoglobin
444 complexes by macrophages, and may also function as an innate immune sensor of
445 bacteria [64].

446 One of the largest macrophage populations in the body occupies the lamina
447 propria of the small and large intestine [65]. They are so numerous that the
448 expression of macrophage-related genes can be detected within the total mRNA
449 from intestine samples. As noted previously in the pig, one can infer from the

450 expression profiles that certain genes that are highly-expressed in AMs are
451 repressed in the intestinal wall [6]. We proposed that such genes, which included
452 many c-type lectins and other receptors involved in bacterial recognition, were
453 necessary for the elimination of inhaled pathogens, where such responses would be
454 undesirable in the gut [6]. In the sheep, there was no large cohort of receptors that
455 showed elevated expression in AMs relative to MDMs or BMDMs, and that were
456 absent in the gut wall. Only a small cluster (115) of 13 genes showed that profile,
457 including the phagocytic receptor *VSIG4* (CRiG), which is a known strong negative
458 regulator of T-cell proliferation and *IL2* production [66] and *SCIMP*, recently identified
459 as a novel adaptor of Toll-like receptor signaling that amplifies inflammatory cytokine
460 production [67]. Six previously unannotated genes within this small cluster included
461 the E3 ubiquitin ligase, *MARCH1*, and likely members of the paired immunoglobulin
462 type receptor and SIGLEC families, which cannot be definitively assigned as
463 orthologues.

464 Interestingly, macrophage colony-stimulating factor receptor (*CSF1R*), which
465 controls the survival, proliferation and differentiation of macrophage lineage cells [68,
466 69], was not within the macrophage-specific cluster 5. Instead, *CSF1R* was in a
467 small cluster (cluster 102) along with several other macrophage-specific genes
468 including the C1Q complex. As in humans and mice [9, 11, 70], *CSF1R* was also
469 expressed in sheep placenta. In humans and mice, placental (trophoblast)
470 expression is directed from a separate promoter [10]. The small number of genes co-
471 expressed with *CSF1R* are likely either co-expressed by trophoblasts as well as
472 macrophages (as is C1Q in humans, see BioGPS
473 (<http://biogps.org/dataset/GSE1133/geneatlas-u133a-qcrma/>) [9, 71]), or highly-
474 expressed in placenta-associated macrophages.

475

476 **Early Development and Reproduction**

477 The sheep gene expression atlas dataset includes multiple libraries from early
478 developmental time points. Three of the larger clusters of co-expressed genes
479 showed high levels of expression in the fetal ovary (cluster 7), fetal brain (cluster 9)
480 and fetal liver (cluster 25). ‘Testis-specific’ genes, particularly those involved in
481 meiosis and gametogenesis, might also be expressed in the fetal ovary undergoing
482 oogenesis [72, 73]. Our dataset from sheep appears to validate this hypothesis,
483 since genes within cluster 7 exhibited higher levels of expression in the fetal ovary
484 and to a lesser extent the testes. Several genes were expressed both in the testes
485 and the fetal ovary including, testis and ovary specific PAZ domain containing 1
486 (*TOPAZ1*), which has been shown in sheep to be expressed in adult male testes and
487 in females during fetal development with a peak during prophase I of meiosis [74].
488 Also, fetal and adult testis expressed 1 (*FATE1*), which is strongly expressed in
489 spermatogonia, primary spermatocytes, and Sertoli cells in seminiferous tubules in
490 mouse and humans [75]. Significantly enriched GO terms for genes within cluster 7
491 included ‘female gonad development’ ($p=4.9 \times 10^{-6}$), ‘spermatogenesis’ ($p=4.6 \times 10^{-8}$)
492 and ‘growth factor activity’ ($p=5 \times 10^{-5}$) (S12 Table).

493 Several important genes for embryonic development were also co-expressed
494 in cluster 7. The germ-cell specific gene SRY-box 30 (*SOX30*) encodes a member of
495 the SOX (SRY-related HMG-box) family of transcription factors involved in the
496 regulation of embryonic development and in the determination of cell fate [76].
497 Growth differentiation factor 3 (*GDF3*) encodes a protein required for normal ocular
498 and skeletal development. Although it is a major stem cell marker gene [77], it has
499 not previously been linked to germ cell expression. Similarly, POU class 5 homeobox

500 1 (*POU5F1*) encodes a transcription factor containing a POU homeodomain that
501 controls embryonic development and stem cell pluripotency [77] but is also required
502 for primordial germ cell survival [78]. The expression of these genes in tissues
503 containing germ cells in sheep suggests they contribute to meiosis and cellular
504 differentiation. These observations illustrate the utility of the sheep as a non-human
505 model for the study of gametogenesis.

506 Cluster 7 also includes two related oocyte-derived members of the
507 transforming growth factor- β (*TGFB1*) superfamily, growth differentiation factor 9
508 (*GDF9*) and bone morphogenetic protein 15 (*BMP15*), which are essential for
509 ovarian follicular growth and have been shown to regulate ovulation rate and
510 influence fecundity in sheep [79, 80]. Lambing rate is an important production trait in
511 sheep and can vary between breeds based on single nucleotide polymorphism
512 (SNP) mutations in key genes influencing ovulation rate [80]. A number of the known
513 fertility genes in sheep (reviewed in [81]), such as the estrogen receptor (*ESR*) and
514 Lacaune gene (*B4GALNT2*) were not present in this cluster 7, which may be
515 because they are not expressed in the ovary at the time points chosen for this study.
516 Detailed analysis of the expression of key genes during early development in the
517 fetal ovary in comparison with the ovary from the adult and gestating ewes may
518 provide additional insights.

519

520 **Sex Specific Differences in Gene Expression**

521 Sex-specific differences in gene expression have been reported in humans
522 [82, 83] mice [84, 85], cattle [86, 87] and pigs [88, 89]. We examined male and
523 female biased gene expression in the sheep atlas dataset by calculating the average
524 TPM per sex for each gene and the female:male expression ratio (S4

525 Supplementary File). Twenty genes exhibited strongly sex biased expression (S16
526 Table); 13 were female-enriched and 7 were male-enriched. Among the male
527 enriched genes was thyroid stimulating hormone beta (*TSHB*), which is expressed in
528 thyrotroph cells in the pituitary gland and part of a neuro-endocrine signaling
529 cascade in sheep [90]. Expression of *TSHB* in the pituitary gland of male BFXT was
530 3.6-fold higher than in female BFXT sheep. A similar sex bias has been observed in
531 rats in which males exhibit significantly higher *TSHB* expression in the pituitary gland
532 than females [91].

533 Other genes exhibiting similarly large sex specific fold-changes included
534 keratin 36 (*KRT36*) which was expressed 6.6-fold higher in the reticulum of male
535 relative to female sheep and *VSIG1* (V-Set and immunoglobulin domain containing
536 1), which is required for the differentiation of glandular gastric epithelia [92]. *VSIG1*
537 showed 4-fold greater expression in the female pylorus relative to the male. An
538 unannotated gene ENSOARG00000020792 exhibited large fold change in male
539 biased expression in immune tissues including popliteal and prescapular lymph
540 node, tonsil and Peyer's patch. This gene has a detectable blast hit to
541 "immunoglobulin kappa-4 light chain variable region" and is a 1:1 orthologue with an
542 unannotated gene in cattle, ENSBTAG00000045514, with $\geq 70\%$ reciprocal
543 percentage identity and conservation of synteny. The dN/dS for
544 ENSOARG00000020792 suggests it is evolving rapidly (dN/dS > 2). Male-biased
545 genes are known to evolve quickly, as are immune genes [93]. GO term enrichment
546 for the set of genes with five-fold sex-biased expression in at least one BFXT tissue
547 (S17 Table) revealed that the genes enriched in females were predominately
548 involved with the immune response while gene enriched in the male were broadly
549 associated with muscle and connective tissue. This is likely to reflect inherent

550 differences between the two sexes in allocation of resources towards growth or
551 immunity. Genes exhibiting sex specific expression might therefore be relevant in
552 sexual dimorphism in disease susceptibility for example, and warrant further
553 investigation.

554

555 **Differential Expression of Genes between the Texel and BFxT**

556 The majority of commercially-produced livestock are a cross of two or more
557 different production breeds with distinct desired traits [94]. For example, in the UK,
558 the crossing of lighter upland sheep breeds with heavier lowland meat breeds
559 optimises carcass quality, lambing rate, growth rate and survivability [94]. In
560 developing countries, sustainable crossing of indigenous small ruminants with elite
561 western breeds is one approach to improve productivity [95, 96]. An RNA-Seq
562 dataset of this size from an outbred cross of two disparate sheep breeds provides an
563 opportunity to investigate differential gene expression in a purebred parental line and
564 crossbred animals. We compared gene expression across tissues in the F₁
565 crossbred (BFxT) animals (generated by crossing a Texel ram with a Scottish
566 Blackface ewe; Fig 5A) with the purebred Texel animals included in the previous
567 sheep gene expression atlas dataset [17].

568 A gene was considered differentially expressed (DE) between the purebred
569 Texel and hybrid BFxT if (a) it was expressed at ≥ 1 TPM in both Texel and BFxT
570 (considering TPM to be the mean of all replicates per tissue), (b) the fold change
571 (ratio of BFxT TPM to Texel TPM) was ≥ 2 in $\geq 25\%$ of the tissues in which expression
572 was detected (stipulating no minimum number of tissues, but noting that 23 tissues
573 are common to Texel and BFxT), and (c) the fold change was ≥ 5 in at least 1 tissue.
574 Fold changes of all genes expressed at ≥ 1 TPM in both breeds are given in S18

575 Table. The GO terms enriched in the set of DE genes (n=772) with higher
576 expression in the BFXT than the Texel were predominantly related either to muscle
577 or brain function (S19 Table). The top 20 genes showing the largest up-regulation
578 (shown as absolute fold-change) in the BFXT relative to the purebred Texel sheep
579 are illustrated in Fig 5B. Enriched molecular function GO terms for the set of genes
580 differentially expressed between BFXT and Texel sheep include 'iron ion binding'
581 ($p=3.6 \times 10^{-4}$), and 'cytoskeletal protein binding' ($p=7.8 \times 10^{-6}$), biological process terms
582 include 'cellular iron ion homeostasis' ($p=6.3 \times 10^{-4}$) and cellular component terms
583 include 'sarcomere' ($p=6.6 \times 10^{-7}$) and 'collagen trimer' ($p=5.5 \times 10^{-7}$) (S19 Table).

584 Numerous genes with structural, motor and regulatory functions were highly
585 expressed in BFXT compared to Texel bicep muscle, with approximately 5- to 18-fold
586 expression increases for various members of the collagen (*COL1A1*, *COL1A2*,
587 *COL3A1*) and myosin families (*MYH2*, *MYL4*), along with *CSRP3* (a
588 mechanosensor) [97], *FMOD* (fibromodulin, a regulator of fibrillogenesis) [98],
589 keratocan (*KERA*, a proteoglycan involved in myoblast differentiation) [99], matrix
590 metalloproteinase 2 (*MMP2*, a proteolytic enzyme associated with muscle
591 regeneration) [100], and calsequestrin 2 (*CASQ2*, one of the most abundant Ca^{2+} -
592 binding proteins in the sarcoplasmic reticulum, essential for muscle contraction)
593 [101].

594 Genes enriched in muscle are of particular biological and commercial interest
595 because Texel sheep exhibit enhanced muscling and less fat [102], due to a single
596 nucleotide polymorphism (SNP) in the 3' untranslated region of the myostatin gene
597 *MSTN* (synonym *GDF-8*) which generates an illegitimate miRNA binding site
598 resulting in translational inhibition of myostatin synthesis and contributing to
599 muscular hypertrophy [23, 103]. Because heterozygotes have an intermediate

600 phenotype, cross breeding of homozygous mutant Texel sheep with animals
601 homozygous for the normal allele transmits something of the Texel muscle
602 phenotype to the offspring. An effect on muscle synthesis in the BFxT animals could
603 be related to the myostatin genotype; genes with higher expression in the Texel than
604 in the cross may be targets for myostatin inhibition [104], while those with lower
605 expression in the Texel than in the cross may be directly or indirectly activated by
606 myostatin and hence involved in the cessation of muscle differentiation. In cattle the
607 myostatin mutation is associated with the downregulation of collagen genes
608 including *COL1A1* and *COL1A2* [104]. This is consistent with the observation that
609 these genes have higher expression in the heterozygous BFxT animals than the
610 Texel animals. Since myostatin also regulates muscle fibre type [105] by
611 suppressing the formation of fast-twitch fibres, individuals homozygous for
612 inactivating myostatin mutations are likely to exhibit increased fast-twitch fibres
613 [106]. Many of the genes up-regulated in the BFxT relative to the Texel animals (e.g.
614 *CSRP3* and *CASQ2*) are known to be specifically expressed in slow-twitch muscle
615 [105, 107], and several down-regulated genes are associated with fast-twitch muscle
616 (e.g. *TNNC2*, *TNNI2* and *SERCA1*) [108, 109]. Consequently, the difference
617 between the cross-breed and pure Texel is in part attributable to an increased
618 contribution of slow-twitch fibres, which in turn has been associated with desirable
619 meat quality traits [110] highlighting the potential advantages of cross-breeding.

620 Enriched GO terms related to brain function include the 'myelin sheath'
621 ($p=6.1 \times 10^{-8}$) and the 'internode region of the axon' ($p=5.2 \times 10^{-5}$) (S19 Table).
622 Candidate genes of particular interest were expressed in the cerebellum (S18
623 Table). For instance, in the BFxT relative to the Texel animals, there were
624 approximately 8-fold expression increases in cochlin (*COCH*, which regulates

625 intraocular pressure) [111] and brevican (*BCAN*, functions throughout brain
626 development in both cell-cell and cell-matrix interactions) [112, 113] and a 10-fold
627 expression increase for myelin-associated oligodendrocyte basic protein, *MOBP*,
628 which was previously unannotated in sheep (ENSOARG00000002491) and has a
629 function in late-stage myelin sheath compaction [114]. A 15-fold expression increase
630 was observed for oligodendrocytic paranodal loop protein (*OPALIN*, a
631 transmembrane protein unique to the myelin sheath [115]), in the BFXT relative to
632 the Texel and a 10-fold increase for another unannotated gene myelin basic protein
633 (*MBP*), which we have assigned to ENSOARG00000004374 [116]. Although these
634 examples of a neuroendocrine-specific effect of cross-breeding are speculative, they
635 are of interest as Scottish Blackface sheep exhibit both improved neonatal
636 behavioural development [117] and more extensive foraging behaviour than lowland
637 breeds such as the Texel, travelling further distances, covering greater areas and
638 exploring higher altitudes [118].

639

640 **Visualisation of the Expression Atlas**

641 We have provided the BFXT sheep gene expression atlas as a searchable
642 database in the gene annotation portal BioGPS
643 (http://biogps.org/dataset/BDS_00015/sheep-atlas/). By searching the dataset via
644 the following link (<http://biogps.org/sheepatlas/>) the expression profile of any given
645 gene can be viewed across tissues. An example profile of the *MSTN* (*GDF-8*)
646 myostatin gene from sheep is included in Fig 6. BioGPS allows comparison of
647 expression profiles across species and links to gene information for each gene [71,
648 119, 120]. The Sheep Atlas BioGPS expression profiles are based on TPM
649 estimates from the alignment-free Kallisto output for the BFXT libraries, averaged

650 across samples from each developmental stage for ease of visualisation. It is
651 important to note that there may be a degree of variation in the expression pattern of
652 individual genes between individuals which is masked when the average profiles are
653 displayed. In addition, to allow comparison between species BioGPS requires each
654 gene have an Entrez ID, which is not the case for all genes in Oar v3.1 and as a
655 consequence these genes do not have visualisable expression profiles in BioGPS.
656 The expression profiles of the genes without Entrez IDs can be found in S1
657 Supplementary File and S2 Supplementary File.

658 In parallel to the alignment-free Kallisto method, we also used an alignment-
659 based approach to RNA-Seq processing, with the HISAT aligner [121] and StringTie
660 assembler [122] (detailed in S3 Supplementary File). These alignments will be
661 published as tracks in the Ensembl genome browser in the short term and integrated
662 into the next Ensembl genome release for sheep.

663

664 **Conclusions**

665 This work describes the transcriptional landscape of the sheep across all
666 major organs and multiple developmental stages, providing the largest gene
667 expression dataset from a livestock species to date. The diversity of samples
668 included in the sheep transcriptional atlas is the greatest from any mammalian
669 species, including humans. Livestock provide an attractive alternative to rodents as
670 models for human conditions in that they are more human-like in their size,
671 physiology and transcriptional regulation, as well as being economically important in
672 their own right. Non-human models are required to study the fundamental biology of
673 healthy adult mammals and as such this dataset represents a considerable new
674 resource for understanding the biology of mammalian tissues and cells.

675 In this sheep transcriptional atlas gene expression was quantified at the gene
676 level across a comprehensive set of tissues and cell-types, providing a starting point
677 for assigning function based on cellular expression patterns. We have provided
678 functional annotation for hundreds of genes that previously had no meaningful gene
679 name using co-expression patterns across tissues and cells. Future analysis of this
680 dataset will use the co-expression clusters to link gene expression to observable
681 phenotypes by highlighting the expression patterns of candidate genes associated
682 with specific traits from classical genetic linkage studies or genome-wide association
683 studies (GWAS). Gene expression datasets have been used in this way to
684 characterise cell populations in mouse [21, 22] and in the biological discovery of
685 candidate genes for key traits in sheep [123-125] and pigs [126, 127]. We have
686 already utilised the dataset to examine the expression patterns of a set of candidate
687 genes linked to mastitis resistance [128] in sheep, including comparative analysis
688 with a recently available RNA-Seq dataset from sheep lactating mammary gland and
689 milk samples [129]. The research community will now be able to use the sheep gene
690 expression atlas dataset to examine the expression patterns of their genes or
691 systems of interest, to answer many of the outstanding questions in ruminant
692 biology, health, welfare and production.

693 Improving the functional annotation of livestock genomes is critical for
694 biological discovery and in linking genotype to phenotype. The Functional Annotation
695 of Animal Genomes Consortium (FAANG) aims to establish a data-sharing and
696 research infrastructure capable of analysing efficiently genome wide functional data
697 for animal species [25, 26]. This analysis is undertaken on a large scale, including
698 partner institutions from across the globe, to further our understanding of how
699 variation in gene sequences and functional components shapes phenotypic diversity.

700 Analysis of these data will improve our understanding of the link between genotype
701 and phenotype, contribute to biological discovery of genes underlying complex traits
702 and allow the development and exploitation of improved models for predicting
703 complex phenotypes from sequence information. The sheep expression atlas is a
704 major asset to genome assembly and functional annotation and provide the
705 framework for interpretation of the relationship between genotype and phenotype in
706 ruminants.

707

708 **Materials and Methods**

709 **Animals**

710 Approval was obtained from The Roslin Institute's and the University of
711 Edinburgh's Protocols and Ethics Committees. All animal work was carried out under
712 the regulations of the Animals (Scientific Procedures) Act 1986. Three male and
713 three female Scottish Blackface x Texel sheep of approximately two years of age
714 were acquired locally and housed indoors for a 7-10 day "settling-in period" prior to
715 being euthanased (electrocution and exsanguination). Nine Scottish Blackface x
716 Texel lambs were born at Dryden Farm Large Animal Unit. Three neonatal lambs
717 were observed at parturition and euthanised immediately prior to their first feed,
718 three lambs were euthanised at one week of age prior to rumination (no grass was
719 present in their GI tract) and three at 8 weeks of age once rumination was
720 established. The lambs were euthanised by schedule one cranial bolt. To obtain
721 developmental tissues six Scottish Blackface ewes were mated to a Texel ram and
722 scanned to ensure successful pregnancy at 21 days. Two were euthanised at 23
723 days, two at 35 days and two at 100 days gestation (electrocution followed by
724 exsanguination). Corresponding time points (day 23, 35 and 100) from gestating

725 BFXT ewes mated with a Texel ram and euthanised as for the Blackface ewes were
726 also included. All the animals, were fed *ad libitum* on a diet of hay and 16% sheep
727 concentrate nut, with the exception of the lambs pre-weaning who suckled milk from
728 their mothers. Details of the animals sampled are included in S1 Table.

729

730 **Tissue Collection**

731 Tissues (95 tissues/female and 93 tissues/male) and 5 cell types were
732 collected from three male and three female adult Scottish Blackface x Texel (BFXT)
733 sheep at two years of age. The same tissues were collected from nine lambs, 3 at
734 birth, 3 at one week and 3 at 8 weeks of age. Three embryonic time points were also
735 included: three day-23 BFXT whole embryos, three BFXT day 35 embryos from
736 which tissue was collected from each region of the basic body plan and three day
737 100 BFXT embryos from which 80 tissues were collected. Reproductive tissue from
738 the corresponding time points from 6 BFXT ewes, 2 at each gestational time point,
739 was also collected. In addition, 3 pools of 8 day 7 blastocysts from abattoir derived
740 oocytes (of unknown breed) fertilized with Texel semen were created using IVF.

741 The majority of tissue samples were collected into RNAlater (AM7021;
742 Thermo Fisher Scientific, Waltham, USA) and a subset were snap frozen, including
743 lipid rich tissues such as adipose and brain. To maintain RNA integrity all tissue
744 samples were harvested within an hour from the time of death. A detailed list of the
745 tissues collected and sequenced can be found in S2 Table. Within the scope of the
746 project we could not generate sequence data from all the samples collected and
747 have archived the remainder for future analysis. Sample metadata, conforming to the
748 FAANG Consortium Metadata standards, for all the samples collected for the sheep
749 gene expression atlas project has been deposited in the BioSamples database

750 under project identifier GSB-718
751 (<https://www.ebi.ac.uk/biosamples/groups/SAMEG317052>).

752

753 **Isolation of Cell Types**

754 All cell types were isolated on the day of euthanasia. Bone marrow cells were
755 isolated from 10 posterior ribs as detailed for pig [130]. BMDMs were obtained by
756 culturing bone marrow cells for 7 days in complete medium: RPMI 1640, Glutamax
757 supplement (35050-61; Invitrogen, Paisley, U.K.), 20% sheep serum (S2263; Sigma
758 Aldrich, Dorset, U.K), penicillin/streptomycin (15140; Invitrogen) and in the presence
759 of recombinant human CSF-1 (rhCSF-1: 10^4 U/ml; a gift of Chiron, Emeryville, CA)
760 on 100-mm² sterile petri dishes, essentially as described previously for pig [130]. For
761 LPS stimulation the resulting macrophages were detached by vigorous washing with
762 medium using a syringe and 18-g needle, washed, counted, and seeded in tissue
763 culture plates at 10^6 cells/ml in CSF-1-containing medium. The cells were treated
764 with LPS from *Salmonella enterica* serotype minnesota Re 595 (L9764; Sigma-
765 Aldrich) at a final concentration of 100 ng/ml as previously described in pig [130] and
766 harvested into TRIzol[®] (Thermo Fisher Scientific) at 0, 2, 4, 7 and 24 h post LPS
767 treatment before storing at -80°C for downstream RNA extraction.

768 PBMCs were isolated as described for pig [131]. MDMs were obtained by
769 culturing PBMCs for 7 days in CSF-1-containing medium, as described above for
770 BMDMs, and harvesting into TRIzol[®] (Thermo Fisher Scientific). Alveolar
771 macrophages were obtained by broncho-alveolar lavage of the excised lungs with
772 500ml sterile PBS (Mg²⁺ Ca²⁺ free) (P5493; Sigma Aldrich). The cells were kept on
773 ice until processing. To remove surfactant and debris cells were filtered through
774 100uM cell strainers and centrifuged at 400 × g for 10 min. The supernatant was

775 removed and 5ml red blood cell lysis buffer (420301; BioLegend, San Diego, USA)
776 added to the pellet for 5 min; then the cells were washed in PBS (Mg^{2+} Ca^{2+} free)
777 (P5493; Sigma Aldrich) and centrifuged at $400 \times g$ for 10 min. The pellet was
778 collected, resuspended in sterile PBS (Mg^{2+} Ca^{2+} free) (Sigma Aldrich), and counted.
779 Alveolar macrophages were seeded in 6-well tissue culture plates in 2ml complete
780 medium: RPMI 1640, Glutamax supplement (35050-61; Invitrogen), 20% sheep
781 serum (S2263; Sigma Aldrich), penicillin/streptomycin (15140; Invitrogen) in the
782 presence of rhCSF1 (10^4 U/ml) overnight.

783 Blood leukocytes were isolated as described in [132]. Whole blood was spun
784 at $500 \times g$ for 10 min (no brake) to separate the buffy coats. These were then lysed
785 in ammonium chloride lysis buffer (150mM NH_4Cl , 10mM $NaHCO_3$, 0.1mM EDTA)
786 for 10 min on a shaking platform, then centrifuged at $4^\circ C$ for 5 min at $500 \times g$. The
787 resultant blood leukocyte pellets were stored in 1ml of RNeasy (Thermo Fisher
788 Scientific) at $-80^\circ C$.

789 To isolate embryonic fibroblasts we harvested a day 35 embryo whole and
790 transferred to outgrowth media (DMEM, high glucose, glutamine, pyruvate (Thermo
791 Fisher Scientific; 11995065), FBS (Fetal Bovine Serum) (Thermo Fisher Scientific;
792 10500056), MEM NEAA (Thermo Fisher Scientific; 11140068),
793 penicillin/streptomycin (Invitrogen), Fungizone (Amphotericin B; Thermo Fisher
794 Scientific; 15290018), Gentamicin (Thermo Fisher Scientific; 15750037)). In a sterile
795 flow hood the head was removed and the body cavity eviscerated. The remaining
796 tissue was washed 3 times in PBS (Mg^{2+} Ca^{2+} free) (Sigma Aldrich) with
797 penicillin/streptomycin (Invitrogen). 5ml of Trypsin-EDTA solution (T4049; Sigma
798 Aldrich) was added and the sample incubated at $37^\circ C$ for 5 min then vortexed and
799 incubated for an additional 5min at $37^\circ C$. 3ml of solution was removed and filtered

800 through a 100uM cell strainer, 5ml of outgrowth media was then passed through the
801 strainer and combined with the sample. The sample was centrifuged at 200 x *g* for 3
802 min and the pellet resuspended in 9ml of out growth media before splitting the
803 sample between 3x T75 flasks. The process then was repeated for remaining 2ml of
804 sample left after the digestion with Trypsin (above). Embryonic fibroblasts were
805 incubated for 5-7 days (until 80-90% confluent) then harvested into TRIzol[®] Reagent
806 (Thermo Fisher Scientific).

807

808 **RNA Extraction and Library Preparation**

809 RNA was extracted using the same method as the Roslin RNA-Seq samples
810 included in the sheep genome project detailed in [17]. For each RNA extraction
811 <100mg of tissue was processed. Care was taken to ensure snap frozen samples
812 remained frozen prior to homogenisation, and any cutting down to the appropriate
813 size was carried out over dry ice. Tissue samples were first homogenised in 1ml of
814 TRIzol[®] reagent (15596018; Thermo Fisher Scientific) with either CK14 (432-3751;
815 VWR, Radnor, USA) or CKMIX (431-0170; VWR) tissue homogenising ceramic
816 beads on a Precellys[®] Tissue Homogeniser (Bertin Instruments; Montigny-le-
817 Bretonneux, France). Homogenisation conditions were optimised for tissue type but
818 most frequently 5000 rpm for 20 sec. Cell samples which had previously been
819 collected in TRIzol[®] Reagent (15596018; Thermo Fisher Scientific), were mixed by
820 pipetting to homogenise. Homogenised (cell/tissue) samples were then incubated at
821 room temperature for 5 min to allow complete dissociation of the nucleoprotein
822 complex, 200µl BCP (1-bromo-3-chloropropane) (B9673; Sigma Aldrich) was added,
823 then the sample was shaken vigorously for 15 sec and incubated at room
824 temperature for 3 min. The sample was centrifuged for 15 min at 12,000 x *g*, at 4°C

825 to separate the homogenate into a clear upper aqueous layer (containing RNA), an
826 interphase and red lower organic layers (containing the DNA and proteins), for three
827 min. DNA and trace phenol was removed using the RNeasy Mini Kit (74106; Qiagen
828 Hilden, Germany) column purification, following the manufacturers instructions
829 (Protocol: Purification of Total RNA from Animal Tissues, from step 5 onwards). RNA
830 quantity was measured using a Qubit RNA BR Assay kit (Q10210; Thermo Fisher
831 Scientific) and RNA integrity estimated on an Agilent 2200 TapeStation System
832 (Agilent Genomics, Santa Clara, USA) using the RNA Screentape (5067-5576;
833 Agilent Genomics) to ensure RNA quality was of RIN^e > 7.

834 RNA-Seq libraries were prepared by Edinburgh Genomics (Edinburgh
835 Genomics, Edinburgh, UK) and run on the Illumina HiSeq 2500 sequencing platform
836 (Illumina, San Diego, USA). Details of the libraries generated can be found in S2
837 Table. A subset of 10 tissue samples and BMDMs at 0 h and 7h (+/-LPS) (Table 1),
838 from each individual, were sequenced at a depth of >100 million strand-specific
839 125bp paired-end reads per sample using the standard Illumina TruSeq total RNA
840 library preparation protocol (Illumina; Part: 15031048, Revision E). These samples
841 were chosen to include the majority of transcriptional output, as in [133]). An
842 additional 40 samples from the tissues and cell types collected per individual
843 (44/female and 42/male), were selected and sequenced at a depth of >25 million
844 strand-specific paired-end reads per sample using the standard Illumina TruSeq
845 mRNA library preparation protocol (poly-A selected) (Illumina; Part: 15031047
846 Revision E).

847 In addition to the samples from the 6 adults, tissue was also collected from
848 other developmental time points. The GI tract tissues collected from the 9 BFXT
849 lambs, 3 at birth, 3 at one week of age and 3 at 8 weeks of age were sequenced at a

850 depth of >25 million reads per sample using the Illumina mRNA TruSeq library
851 preparation protocol (poly-A selected) as above. Of the early developmental time
852 points, the three 23 day old embryos from BFxT sheep were sequenced at >100
853 million reads using the Illumina total RNA TruSeq library preparation protocol (as
854 above), while the other embryonic samples and the ovary and placenta from the
855 gestating ewes were sequenced at a depth of >25 million reads per sample using the
856 Illumina mRNA TruSeq library preparation protocol (as above). In addition, three
857 libraries were generated using the NuGen Ovation Single Cell RNA-Seq System
858 (0342-32-NUG; NuGen, San Carlos, USA) from pooled samples of 8 blastocysts (as
859 in [134]), and sequenced at a depth of >60 million reads per sample. A detailed list of
860 prepared libraries, including library type can be found in S2 Table.

861 To identify spurious samples we used sample-to-sample correlation, of the
862 transposed data from S1 Supplementary File, in Miru (Kajeka Ltd) [38]. The sample-
863 to-sample graph is presented in S2 Fig. The expression profiles of any samples
864 clustering unexpectedly (i.e. were not found within clusters of samples of the same
865 type/biological replicate) were examined in detail. Generally the correlation between
866 samples was high, although 4 spurious samples and 4 sets of swapped samples
867 were identified. These samples were either relabeled or removed as appropriate.

868

869 **Data Quality Control and Processing**

870 Raw data is deposited in the European Nucleotide Archive under study
871 accession number PRJEB19199 (<http://www.ebi.ac.uk/ena/data/view/PRJEB19199>).
872 The RNA-Seq data processing methodology and pipelines are described in detail in
873 S3 Supplementary File. For each tissue a set of expression estimates, as transcripts
874 per million (TPM), were obtained using the high speed transcript quantification tool

875 Kallisto [28]. In total, the expression atlas utilised approximately 26 billion (pseudo)
876 alignments (S3 Table), capturing a large proportion of protein-coding genes per
877 tissue (S20 Table).

878 The accuracy of Kallisto is dependent on a high quality index (reference
879 transcriptome) [28], so in order to ensure an accurate set of gene expression
880 estimates we employed a ‘two-pass’ approach. We first ran Kallisto on all samples
881 using as its index the Oar v3.1 reference transcriptome. We then parsed the
882 resulting data to revise this index. This was in order to include, in the second index,
883 those transcripts that should have been there but were not (i.e. where the reference
884 annotation is incomplete), and to remove those transcripts that should not be there
885 but were (i.e. where the reference annotation is poor quality and a spurious model
886 has been introduced). For the first criterion, we obtained the subset of reads that
887 Kallisto could not align, assembled those *de novo* into putative transcripts (S3
888 Supplementary File), then retained each transcript only if it could be robustly
889 annotated (by, for instance, encoding a protein similar to one of known function) and
890 showed coding potential (S21 Table). For the second criterion, we identified those
891 members of the reference transcriptome for which no evidence of expression could
892 be found in any of the hundreds of samples comprising the atlas. These were then
893 discarded from the index. Finally, this revised index was used for a second iteration
894 of Kallisto, generating higher-confidence expression level estimates. This improved
895 the capture rate of protein-coding genes (S22 Table). A detailed description of this
896 process can be found in S3 Supplementary File.

897 We complemented this alignment-free method with a conventional alignment-
898 based approach to RNA-Seq processing, using the HISAT aligner [121] and
899 StringTie assembler [122]. A detailed description of this pipeline is included in S3

900 Supplementary File. This assembly is highly accurate with respect to the existing
901 (Oar v3.1) annotation, precisely reconstructing almost all exon (96%), transcript
902 (98%) and gene (99%) models (S23 Table). Although this validates the set of
903 transcripts used to generate the Kallisto index, we did not use HISAT/StringTie to
904 quantify expression. This is because a standardised RNA space is necessary to
905 compare data from mRNA-Seq and total RNA-Seq libraries [30], which cannot be
906 applied if expression is quantified via genomic alignment. Unlike alignment-free
907 methods, however, HISAT/StringTie can be used to identify novel transcript models
908 (S24 Table), particularly for ncRNAs, which will be described in detail in a dedicated
909 analysis. We will publish the alignments from HISAT and Stringtie as tracks in the
910 Ensembl genome browser in the short term and integrate the alignments into
911 Ensembl and Biomart in the next Ensembl release for sheep.

912

913 **Inclusion of Additional RNA-Seq Datasets from Sheep**

914 Additional RNA-Seq data was obtained from a previous characterisation of
915 the transcriptome of 3 Texel sheep included in the release of the current sheep
916 genome Oar v3.1 [17]. The dataset included tissues from an adult Texel ram (n=29),
917 an adult Texel ewe (n=25) and their female (8-9 month old) lamb (n=28), plus a
918 whole embryo (day 15 gestation) from the same ram-ewe pairing. The raw read data
919 from the 83 Texel samples incorporated into this dataset and previously published in
920 [17] is located in the European Nucleotide Archive (ENA) study accession
921 PRJEB6169 (<http://www.ebi.ac.uk/ena/data/view/PRJEB6169>). The metadata for
922 these individuals is included in the BioSamples database under Project Identifier
923 GSB-1451 (<https://www.ebi.ac.uk/biosamples/groups/SAMEG317052>). A small
924 proportion of the tissues included in the Texel RNA-Seq dataset were not sampled in

925 the BFXT gene expression atlas. Those unique to the Texel are largely drawn from
926 the female reproductive, integument and nervous systems: cervix, corpus luteum,
927 ovarian follicles, hypothalamus, brain stem, omentum and skin (side and back).
928 Details of the Texel RNA-Seq libraries including tissue and cell type are included in
929 S25 Table. The Texel samples were all prepared using the Illumina TruSeq stranded
930 total RNA protocol with the Ribo-Zero Gold option for both cytoplasmic and
931 mitochondrial rRNA removal, and sequenced using the Illumina HiSeq 2500 (151bp
932 paired-end reads) [17]. As above, Kallisto was used to estimate expression level for
933 all samples, using the revised reference transcriptome (from the ‘second pass’) as its
934 index.

935

936 **Correcting for the Effect of Multiple Library Types**

937 To correct for the confounding effect of multiple library types we applied a
938 batch effect correction. We have previously validated this method using a subset of
939 the sheep atlas expression atlas samples from BMDMs (+/- LPS) sequenced both as
940 mRNA and total RNA libraries [30]. As described above, for the Kallisto second
941 pass, we constrained the Kallisto index to contain only the transcripts of protein-
942 coding genes, pseudogenes and processed pseudogenes, the majority of which are
943 poly(A)+ and so are present in both mRNA-Seq and total RNA-Seq samples. We
944 then calculated, per gene, the ratio of mean TPM across all mRNA-Seq libraries to
945 mean TPM across all total RNA-Seq libraries. Given the scope of the tissues
946 sampled for both library types (all major organ systems from both sexes and from
947 different developmental states), neither mean is likely to be skewed by any tissue-
948 specificity of expression. As such, any deviations of this ratio from 1 will reflect
949 variance introduced by library type/depth. Thus, to correct each gene’s set of

950 expression estimates for this effect of library type, we multiplied all total RNA-Seq
951 TPMs by this ratio. To validate this approach we used principal component bi-plot
952 analysis, described and shown in S3 Supplementary File and S1 Fig.

953

954 **Gene Expression, Network Cluster Analysis and Annotation**

955 Network cluster analysis of the sheep gene expression atlas was performed
956 using Miru (Kajeka Ltd, Edinburgh, UK) [36-38]. In brief, similarities between
957 individual gene expression profiles were determined by calculating a Pearson
958 correlation matrix for both gene-to-gene and sample-to-sample comparisons, and
959 filtering to remove relationships where $r < 0.75$. A network graph was constructed by
960 connecting the remaining nodes (genes) with edges (where the correlation exceeded
961 the threshold value). This graph was interpreted by applying the Markov Cluster
962 algorithm (MCL) [39] at an inflation value (which determines cluster granularity) of
963 2.2. The local structure of the graph was then examined visually. Genes with robust
964 co-expression patterns, implying related functions, clustered together, forming
965 cliques of highly interconnected nodes. A principle of ‘guilt by association’ was then
966 applied, i.e. the function of an unannotated gene could be inferred from the genes it
967 clustered with [19, 135]. Expression profiles for each cluster were examined in detail
968 to understand the significance of each cluster in the context of the biology of sheep
969 tissues and cells. Clusters 1 to 50 (Table 2) were assigned a functional ‘class’ and
970 ‘sub-class’ manually by first determining if multiple genes within a cluster shared a
971 similar biological function based on both gene ontology [40], determined using the
972 Bioconductor package ‘topGO’ [136] (GO term enrichment for clusters 1 to 50 is
973 shown in S12 Table). We then compared the clusters with tissue- and cell-specific
974 clusters in other large-scale network-based gene expression analyses including the

975 pig gene expression atlas [6], the human protein atlas [70, 73, 137] and the mouse
976 atlas [9, 138, 139]. More specific annotation of the GI tract clusters in sheep was
977 based on network and pathway analysis from the sheep genome paper and a
978 subsequent satellite publication [17, 20]. The gene component of all clusters can be
979 found in S11 Table.

980 We assigned gene names to unannotated genes in Oar v3.1 based on their
981 co-expression pattern, tissue specificity, and reciprocal percent identity to a set of
982 nine known ruminant proteomes (S7 Table). The annotation pipeline is described in
983 detail in S3 Supplementary File and included a set of quality categories summarised
984 in S5 Table. We were able to assign gene names to >1000 previously unannotated
985 genes in Oar v3.1. Candidate gene names are given as both a shortlist (S8 Table)
986 and a longlist (S9 Table), the latter intended for manual review as informative
987 annotations may still be made without every one of the above criteria being met.

988

989 **Table 1: Details of the tissues and cell types sequenced to generate the BFXT**
990 **RNA-Seq dataset for the sheep gene expression atlas.** Tissues and cells were
991 chosen to cover all major organ systems. All libraries were Illumina 125bp paired
992 end stranded libraries. See S2 Table for a detailed list of the tissues and cell types
993 sequenced.

994

Subset	Tissue Type	Library Type	Sequencing Depth	Total Number of Libraries	Number of Individuals
Core Atlas	Liver, spleen, ovary, testes, hippocampus, kidney medulla, bicep muscle, reticulum, ileum, thymus, left ventricle	Total RNA-Seq	>100 million reads per sample	60 (10 per individual)	3 adult males and 3 adult females

Core Atlas	GI tract, reproductive tract, brain, endocrine, cardiovascular, lymphatic, musculo-skeletal, immune cells	mRNA-Seq	>25 million reads per sample	248 (~45 per individual)	3 adult males and 3 adult females
LPS Time Course (Core Atlas)	BMDM 0h (-LPS) and 7h (+LPS)	Total RNA-Seq	>100 million reads per sample	12 (2 time points per individual)	3 adult males and 3 adult females
LPS Time Course (Core Atlas)	BMDM 2h, 4h, 24h post LPS treatment	mRNA-Seq	>25 million reads per sample	32 (3 time points per individual)	3 adult males and 3 adult females
GI Tract Time Series	Gastro-intestinal tract	mRNA-Seq	>25 million reads per sample	90 (10 tissues per individual)	9 lambs (3 at birth, 3 at one week and 3 at 8 weeks)
Early Development (blastocysts)	Day 7 blastocysts (3 pools of 8)	Nu Gen Single Cell Ovation Kit	>66 million reads per sample	3	3 pools
Early Development (day 23)	Day 23 whole embryos	Total RNA-Seq	>100 million reads per sample	3	3
Early Development (day 35)	Liver, brain, embryonic fibroblasts	mRNA-Seq	>25 million reads per sample	7	3 embryos (two female and one male)
Early Development (day 100)	Liver, ovary	mRNA-Seq	>25 million reads per sample	5	3 female (liver) 2 female (ovary)
Maternal Reproductive Time Series (days, 23, 35 and 100)	Placenta and ovary	mRNA-Seq	>25 million reads per sample	12	2 females per time point

995

996 **Table 2: The number and percentage of Oar v3.1 protein coding and non-**
 997 **coding genes, with average TPM across all animals > 1 in at least one tissue,**
 998 **in both the BFXt dataset after the Kallisto first and second pass, and after**
 999 **incorporating the existing Texel dataset. 'BFXt data' refers to the present study;**
 1000 'Texel data' is obtained from [17]. The 'first pass' Kallisto index contains the known
 1001 *Ovis aries* v3.1 cDNAs for both protein-coding and non-protein coding transcripts.
 1002 The 'second pass' Kallisto index is a filtered version of the former, that (a) restricts

1003 the RNA space to protein-coding genes, pseudogenes, and processed pseudogenes
 1004 (so that expression within an equivalent space will be quantified, irrespective of
 1005 experimental protocol), (b) omits genes that had no detectable expression across all
 1006 BFXt samples, and (c) includes novel transcript reconstructions further to the *de*
 1007 *novo* assembly of unmapped reads.
 1008

RNA-Seq data used:	Scottish Blackface x Texel Libraries Only					Including the existing Texel dataset	
	First-Pass			Second-Pass (restricted)		Second-Pass (restricted)	
Kallisto index:	No. in reference annotation (Oar v3.1)	No. of genes of this type expressed	% genes of this type expressed	No. of genes of this type expressed	% genes of this type expressed	No. of genes of this type expressed	% genes of this type expressed
lincRNA	1858	1548	83.32	0	0	0	0
miRNA	1305	1242	95.17	0	0	0	0
misc RNA	361	310	85.87	0	0	0	0
MT rRNA	2	2	100	0	0	0	0
MT tRNA	22	19	86.36	0	0	0	0
processed pseudogene	43	31	72.09	35	81.40	38	88.37
protein-coding	20921	19921	95.22	20189	96.50	20359	97.31
pseudogene	247	172	69.64	189	76.52	201	81.38
rRNA	305	272	89.18	0	0	0	0
snoRNA	756	717	94.84	0	0	0	0
snRNA	1234	1116	90.44	0	0	0	0
Sum	27054	25350		20413		20598	

1009

1010 **Table 3: Tissue/cell/pathway association of the largest 50 network clusters in**
 1011 **the sheep gene expression atlas dataset.**

Cluster ID	Number of Transcripts	Profile Description	Class	Sub-Class
1	1199	General	House Keeping	House Keeping (1)
2	987	Brain	CNS	CNS
3	658	Testes – Adult	Reproduction	Gamete Production
4	585	General	House Keeping	House Keeping (2)
5	351	Macrophages	Immune	Macrophages
6	350	Fallopian Tube > Testes	Cilia	Motile Cilia
7	284	Fetal Ovary > Adult Testes	Early Development	Reproduction
8	276	Many Tissues - Highly Variable	Pathway	Cell Cycle
9	265	Fetal Brain > Adult Brain	CNS	CNS
10	247	Skeletal Muscle > Oesophageal Muscle	Musculature	Skeletal Muscle
11	219	Lymph Nodes > Blood > Not Macrophages	Immune	T-Cell and B-Cell
12	215	Thymus > Salivary Gland	Immune	T-Cell
13	186	Fore-Stomachs > Tonsil > Skin	GI Tract	Ruminal Epithelium
14	183	Kidney Cortex > Liver	Renal	Kidney Cortex
15	182	General but not even - highest in muscle	Pathway	Oxidative Phosphorylation
16	158	Epididymis > Vas Deferens	Reproduction	Male
17	153	Liver	Liver	Liver (Hepatocytes)
18	145	Peyer's Patch, Ileum, Lymph Nodes, Blood	Immune	T-Cell and B-Cell
19	134	Placenta	Gestation	Placental Function
20	119	Epididymis > Testes > Vas Deferens	Reproduction	Male
21	115	General but not even	Pathway	Ribosomal
22	102	Adrenal Gland	Endocrine	Steroid Hormone Biosynthesis
23	102	Placenta	Gestation	Placental Function
24	98	Liver > Small Intestine	Liver	Liver (GI Tract)
25	96	Fetal Liver	Liver	Developing Liver
26	92	Small Intestine > Large Intestine	GI tract	GI Tract
27	90	Pituitary Gland	Endocrine	Hormone Synthesis
28	85	General highest in reproductive tissues and brain	Cilia	Primary Cilia
29	77	Heart	Musculature	Cardiac Muscle
30	75	Thyroid	Endocrine	Thyroxine Synthesis
31	73	Peyers Patch, Ileum, Lymph Nodes, Blood, Macrophages	Immune	T-Cell and B-Cell
32	69	Salivary Gland, Lymph Node, Blood, Small Intestine	Immune	T-Cell and B-Cell

33	68	Fore-Stomachs Adult - Not Neonates > AMs	GI Tract	Immune
34	65	Small Intestine > Large Intestine	GI tract	GI Tract
35	61	General - highest in brain	House Keeping	House Keeping (3)
36	58	Heart Valves	Cardiovascular	Extra Cellular Matrix
37	58	General - highest in blood	House Keeping	House Keeping (4)
38	56	General - highest in fetal brain	House Keeping	House Keeping (5)
39	50	GI Tract - highest in reticulum	GI Tract	GI Tract
40	49	General - highest in testes	House Keeping	House Keeping (6)
41	49	General - highest in ovary	House Keeping	House Keeping (7)
42	47	General - highest in brain	House Keeping	House Keeping (8)
43	45	Fore-Stomachs > Tonsil > Skin	GI Tract	Ruminal Epithelium
44	45	General - highest in testes	House Keeping	House Keeping (9)
45	44	Macrophage (BMDM + LPS)	Immune	Macrophages (LPS Response TNF)
46	44	Blood, Lymph Nodes	Immune	Blood
47	42	Large Intestine	GI Tract	GI Tract
48	42	General	Pathway	Histones
49	41	Reticulum and Rumen - very variable	GI Tract	Reticulum/Rumen
50	36	Adrenal Gland Medulla	Endocrine	Steroid Hormone Biosynthesis

1012

1013 **Fig 1: Hierarchical clustering of the samples included in the sheep gene**
 1014 **expression atlas dataset.** Samples of each tissue and cell type from each breed
 1015 and developmental stage were averaged across individuals for ease of visualisation.
 1016 The tree was constructed from the Euclidean distances between expression vectors
 1017 using MEGA v7.0.14 [31] with the neighbour-joining method and edited in the
 1018 graphical viewer FigTree v1.4.3 [32]. Clustering is biologically meaningful and
 1019 highlights the lack of any significant effect of library type post-correction. Samples
 1020 are coloured by organ system.

1021

1022 **Fig 2: Network visualisation and clustering of the sheep gene expression atlas.**

1023 A three-dimensional visualisation of a Pearson correlation gene-to-gene graph of
1024 expression levels derived from RNA-Seq data from analysis of sheep tissues and
1025 cells. Each node (sphere) in the graph represents a gene and the edges (lines)
1026 correspond to correlations between individual measurements above the defined
1027 threshold. The graph is comprised of 15,192 nodes (genes) and 811,213 edges
1028 (correlations ≥ 0.75). Co-expressed genes form highly connected complex clusters
1029 within the graph. Genes were assigned to groups according to their level of co-
1030 expression using the MCL algorithm.

1031

1032 **Fig 3: Collapsed node visualisation of the sheep gene expression atlas**
1033 **dataset in two-dimensions to illustrate the relative proportion of genes in each**

1034 **cluster.** Includes 3104 nodes and 138,407 edges with a Pearson correlation value of
1035 $r=0.75$ and an MCL inflation (MCLi) value of 2.2. Nodes are coloured by tissue/cell
1036 type or for broader classes organ system. The largest clusters are numbered from 1
1037 to 30 (see Table 3 for functional annotation). The largest clusters are dominated by
1038 either house-keeping genes (1 & 4) or genes associated with transcriptionally rich
1039 tissues or cell types, such as brain (2), testes (3) and macrophages (5).

1040

1041 **Fig 4: Interrogation of the underlying expression profiles allows regions of the**
1042 **graph to be associated with specific tissues or cell types. A**

1043 visualisation of a Pearson correlation gene to gene network graph ($r=0.75$,
1044 MCLi=2.2). Samples of each tissue and cell type from each breed and
1045 developmental stage are averaged across individuals for ease of visualisation.
1046 Histograms of the averaged expression profile (averaged across individuals for each

1047 tissue and cell type for ease of visualisation) of genes in selected clusters are given
1048 on the right: **B (i)** profile of cluster 5 genes whose expression is highest in
1049 macrophages; **(ii)** profile of cluster 7 genes whose expression is highest in fetal
1050 ovary and testes; **(iii)** or a broader expression pattern associated with a cellular
1051 process e.g. oxidative phosphorylation (cluster 15). Note that there may be a degree
1052 of variation in the expression pattern of individual genes within a cluster which is
1053 masked when average profiles are displayed.

1054

1055 **Fig 5: Upregulation of genes in the crossbred BFxT relative to the purebred**
1056 **Texel. A** A Texel sire was crossed with Scottish Blackface dam to create the F1
1057 Texel x Scottish Blackface individuals. **B** The top 20 genes showing the greatest up-
1058 regulation (as absolute fold change) between the crossbred BFxT and purebred
1059 Texel individuals. Genes associated with the function of skeletal muscle and
1060 connective tissue are indicated.

1061

1062 **Fig 6: Screenshot of the representation of the profile of the sheep *GDF-8***
1063 **(*MSTN*) gene within the BioGPS online portal.** All data from the BFxT sheep gene
1064 expression atlas dataset are available through the BioGPS database
1065 (http://biogps.org/dataset/BDS_00015/sheep-atlas/). This provides a searchable
1066 database of genes, with expression profiles across tissues and cells for each gene
1067 displayed as histograms (<http://biogps.org/sheepatlas/>). Samples are coloured
1068 according to organ system, for example, Immune, GI Tract etc. The BioGPS platform
1069 supports searching for genes with a similar profile, allows access to the raw data,
1070 and links to external resources. It also provides the potential for comparative
1071 analysis across species, for example with the expression profiles for pig.

1072 **Supplemental Material**

1073

1074 **S1 Fig: Principal component analysis with all samples plotted in two**
1075 **dimensions using their projections onto the first two principal components.**

1076 For each sample, each gene's expression level is taken as the mean TPM across all
1077 replicates, before **(A)** and after **(B)** any batch effect correction. Samples are coloured
1078 by organ system. Ellipses indicate confidence intervals of 95%. The shape of each
1079 point indicates each sample's library type: mRNA-seq (circle) or total RNA-seq
1080 (triangle). Blastocyst samples are excluded for clarity as they are generated using a
1081 different experimental protocol. Before correction, points can be partitioned by shape
1082 (to the left and right of sub-Fig A), suggesting a batch effect – variation introduced by
1083 library type confounds variation by tissue type. After correction (sub-Fig B), there is
1084 no notable axis of variation that partitions points by shape – consequently, variation
1085 introduced by library type (a batch effect) does not confound variation by tissue type
1086 (which is biologically meaningful).

1087

1088 **S2 Fig: Sample-to-sample network graph analysis was used to validate the**
1089 **samples included in the sheep gene expression atlas dataset.** Each node

1090 represents a sample and each edge its connectivity to other samples in the dataset.
1091 A correlation of $r=0.75$ split the graph into 10 different clusters. The largest cluster
1092 (cluster 1) included the majority of samples ('mixed tissues'), most of which were
1093 transcriptionally similar, while the remainder of the clusters comprised samples with
1094 distinctive transcriptional signatures such as macrophages (3) and abomasum.
1095 Spurious samples were easily identified if they were present in a cluster comprised

1096 of samples from a different tissue or cell type. Pearson Correlation $r=0.75$, MCLi =
1097 2.2, nodes = 481 and edges = 23,903.

1098

1099 **S1 Supplementary File:** Gene Expression Level Atlas as transcripts per million
1100 (unaveraged)

1101 **S2 Supplementary File:** Gene Expression Level Atlas as transcripts per million
1102 (averaged across biological replicates for each developmental stage)

1103 **S3 Supplementary File:** Additional Methods

1104 **S4 Supplementary File:** Sex-biased Expression Atlas (based on expression
1105 estimates from 3 adult male and 3 adult female BFXT sheep)

1106

1107 **S1 Table:** Overview of animals used to generate the sheep atlas tissue subsets.

1108 **S2 Table:** Details of library type and tissue/cell samples used in each subset of
1109 samples.

1110 **S3 Table:** Number of reads, and number of aligned reads, per sample.

1111 **S4 Table:** Genes undetected (TPM < 1) in every tissue/cell line of the expression
1112 atlas.

1113 **S5 Table:** Quality categories for automated gene annotations.

1114 **S6 Table:** Proportion of unannotated protein-coding genes assigned probable gene
1115 names.

1116 **S7 Table:** Source of ruminant proteome data.

1117 **S8 Table:** Candidate gene names for unannotated Oar v3.1 protein-coding genes:
1118 shortlist.

1119 **S9 Table:** Candidate gene names for unannotated Oar v3.1 protein-coding genes:
1120 longlist.

1121 **S10 Table:** Candidate gene descriptions for all unannotated Oar v3.1. protein-coding
1122 genes (potentially informative in the absence of a gene name).

1123 **S11 Table:** Genes within each co-expression cluster.

1124 **S12 Table:** GO term enrichment for co-expression clusters 1 to 50.

1125 **S13 Table:** Manual annotation of cluster 15 (genes involved in oxidative
1126 phosphorylation).

1127 **S14 Table:** Manual annotation of unannotated genes in cluster 12 (genes with a T-
1128 cell signature).

1129 **S15 Table:** Manual annotation of unannotated genes in cluster 5 (genes with an
1130 alveolar macrophage signature).

1131 **S16 Table:** Genes with five-fold sex-biased expression in at least one BFxT tissue.

1132 **S17 Table:** GO term enrichment for the set of genes with five-fold sex-biased
1133 expression in at least one BFxT tissue.

1134 **S18 Table:** Fold changes in expression level between BFxT and Texel sheep.

1135 **S19 Table:** GO term enrichment for the set of genes differentially expressed
1136 between BFxT and Texel sheep.

1137 **S20 Table:** Number of genes with detectable expression, per tissue.

1138 **S21 Table:** Coding potential of putative novel CDS.

1139 **S22 Table:** Number of genes with detectable expression, per gene type.

1140 **S23 Table:** Proportion of Oar v3.1 gene, exon and transcript models in the StringTie
1141 assembly.

1142 **S24 Table:** Novel transcript models in the StringTie assembly.

1143 **S25 Table:** Details of the additional RNA-Seq libraries included from Texel sheep
1144 (Jiang, et al. (2014) Science. 344(6188):1168-1173).

1145

1146 **Acknowledgments**

1147 We would like to thank the large number of people at the Roslin Institute who helped
1148 with the many aspects of the sheep atlas project. Douglas McGavin and David
1149 Chisholm coordinated the management of the sheep at Dryden Farm. Tim King,
1150 Peter Tennant, Adrian Ritchie, John Bracken and Pip Beard conducted post
1151 mortems on the animals. The lists of tissues for collection were developed by Erika
1152 Abbondati. Detailed dissection of the brain was performed by Fiona Houston. The
1153 tissue collection team included Heather Finlayson, Christine Burkhard, Alison
1154 Wilson, Ailsa Carlisle, Mark Barnett, Gemma Davis, Anna Raper, Rocio Rojo, Alex
1155 Brown, Chris Proudfoot, Laura Glendinning, Sara Clohisey, Yolanda Corripio-Miyar,
1156 Jack Ferguson, Karen Fernie and Jason Ioannidis. Blood Leukocytes were isolated
1157 by John Hopkins. RNA from the GI Tract was isolated by Gemma Davis and from
1158 embryonic fibroblasts by Charity Muriuki. Library preparation and sequencing was
1159 carried out by Edinburgh Genomics, The University of Edinburgh. We would
1160 also like to thank Norman Russell (The Roslin Institute) for generating the
1161 photographic images used and Andrew Su, Cyrus Afrasiabi and Chunlei Wu for
1162 uploading the data to BioGPS and allowing us to use their platform for visualisation.

1163

1164 **Availability of Data and Materials**

1165 The datasets supporting the conclusions of this article are available in the following
1166 locations. The raw read data for all new BFXT libraries generated for this project is
1167 deposited in the European Nucleotide Archive (ENA) under study accession number
1168 PRJEB19199 (<http://www.ebi.ac.uk/ena/data/view/PRJEB19199>). Sample metadata
1169 for all the tissue and cell samples collected has been deposited in the EBI
1170 BioSamples database under project identifier GSB-718

1171 (<https://www.ebi.ac.uk/biosamples/groups/SAMEG317052>). The raw read data from
1172 the 83 Texel samples incorporated into this dataset and previously published in [17]
1173 is located in the European Nucleotide Archive (ENA) study accession PRJEB6169
1174 (<http://www.ebi.ac.uk/ena/data/view/PRJEB6169>). All experimental protocols are
1175 available on the FAANG consortium ftp site at <http://ftp.faang.ebi.ac.uk/ftp/protocols/>.

1176

1177 **Competing interests**

1178 The authors have declared that no competing interests exist.

1179

1180 **Funding**

1181 The work was supported by a Biotechnology and Biological Sciences Research
1182 Council (BBSRC) Grant BB/L001209/1 ('Functional Annotation of the Sheep
1183 Genome'), Institute Strategic Program Grants Farm Animal Genomics
1184 (BBS/E/D/20211550) and Transcriptomes, Networks and Systems
1185 (BBS/E/D/20211552) and a National Capability Grant (ARK-Genomics,
1186 BBS/E/D/20310000). Edinburgh Genomics is partly supported through core
1187 grants from NERC (R8/H10/56), MRC (MR/K001744/1) and BBSRC
1188 (BB/J004243/1). SB was supported by the Roslin Foundation.

1189

1190 **References**

1191

1192 1. Marino R, Atzori AS, D'Andrea M, Iovane G, Trabalza-Marinucci M, Rinaldi L.
1193 Climate change: Production performance, health issues, greenhouse gas emissions
1194 and mitigation strategies in sheep and goat farming. *Small Ruminant Research*.
1195 2016;135:50-9. doi: doi.org/10.1016/j.smallrumres.2015.12.012.

- 1196 2. Brito LF, Clarke SM, McEwan JC, Miller SP, Pickering NK, Bain WE, et al.
1197 Prediction of genomic breeding values for growth, carcass and meat quality traits in
1198 a multi-breed sheep population using a HD SNP chip. *BMC Genetics*. 2017;18(1):7.
1199 doi: 10.1186/s12863-017-0476-8.
- 1200 3. Hayes BJ, Lewin HA, Goddard ME. The future of livestock breeding: genomic
1201 selection for efficiency, reduced emissions intensity, and adaptation. *Trends in*
1202 *Genetics*. 2013;29(4):206-14. doi: doi.org/10.1016/j.tig.2012.11.009.
- 1203 4. Daetwyler HD, Hickey JM, Henshall JM, Dominik S, Gredler B, van der Werf
1204 JHJ, et al. Accuracy of estimated genomic breeding values for wool and meat traits
1205 in a multi-breed sheep population. *Animal Production Science*. 2010;50(12):1004-10.
1206 doi: doi.org/10.1071/AN10096.
- 1207 5. Wickramasinghe S, Cánovas A, Rincón G, Medrano JF. RNA-Sequencing: A
1208 tool to explore new frontiers in animal genetics. *Livestock Science*. 2014;166:206-16.
1209 doi: doi.org/10.1016/j.livsci.2014.06.015.
- 1210 6. Freeman TC, Ivens A, Baillie JK, Beraldi D, Barnett MW, Dorward D, et al. A
1211 gene expression atlas of the domestic pig. *BMC Biology*. 2012;10(1):90. doi:
1212 10.1186/1741-7007-10-90.
- 1213 7. Harhay GP, Smith TP, Alexander LJ, Haudenschild CD, Keele JW,
1214 Matukumalli LK, et al. An atlas of bovine gene expression reveals novel distinctive
1215 tissue characteristics and evidence for improving genome annotation. *Genome*
1216 *Biology*. 2010;11(10):R102. doi: 10.1186/gb-2010-11-10-r102.
- 1217 8. Su AI, Cooke MP, Ching KA, Hakak Y, Walker JR, Wiltshire T, et al. Large-
1218 scale analysis of the human and mouse transcriptomes. *Proc Natl Acad Sci USA*.
1219 2002;99. doi: 10.1073/pnas.012025199.

- 1220 9. Su AI, Wiltshire T, Batalov S, Lapp H, Ching KA, Block D, et al. A gene atlas
1221 of the mouse and human protein-encoding transcriptomes. *Proc Natl Acad Sci USA*.
1222 2004;101. doi: 10.1073/pnas.0400782101.
- 1223 10. Andersson R, Gebhard C, Miguel-Escalada I, Hoof I, Bornholdt J, Boyd M, et
1224 al. An atlas of active enhancers across human cell types and tissues. *Nature*.
1225 2014;507(7493):455-61. doi: doi.org/10.1038/nature12787.
- 1226 11. Lizio M, Harshbarger J, Shimoji H, Severin J, Kasukawa T, Sahin S, et al.
1227 Gateways to the FANTOM5 promoter level mammalian expression atlas. *Genome*
1228 *Biology*. 2015;16(1):22. doi: 10.1186/s13059-014-0560-6.
- 1229 12. Forrest AR, Kawaji H, Rehli M, Baillie JK, De Hoon M, Haberle V, et al. A
1230 promoter-level mammalian expression atlas. *Nature*. 2014;507(7493):462-70. doi:
1231 doi.org/10.1038/nature13182.
- 1232 13. Birney E, Stamatoyannopoulos JA, Dutta A, Guigo R, Gingeras TR, Margulies
1233 EH, et al. Identification and analysis of functional elements in 1% of the human
1234 genome by the ENCODE pilot project. *Nature*. 2007;447. doi: 10.1038/nature05874.
- 1235 14. Melé M, Ferreira PG, Reverter F, DeLuca DS, Monlong J, Sammeth M, et al.
1236 The human transcriptome across tissues and individuals. *Science*.
1237 2015;348(6235):660. doi: 10.1126/science.aaa0355.
- 1238 15. Bickhart DM, Rosen BD, Koren S, Sayre BL, Hastie AR, Chan S, et al. Single-
1239 molecule sequencing and chromatin conformation capture enable de novo reference
1240 assembly of the domestic goat genome. *Nat Genet*. 2017;49(4):643-50. doi:
1241 doi.org/10.1038/ng.3802.
- 1242 16. Worley KC. A golden goat genome. *Nat Genet*. 2017;49(4):485-6. doi:
1243 10.1038/ng.3824.

- 1244 17. Jiang Y, Xie M, Chen W, Talbot R, Maddox JF, Faraut T, et al. The sheep
1245 genome illuminates biology of the rumen and lipid metabolism. *Science*.
1246 2014;344(6188):1168. doi: 10.1126/science.1252806.
- 1247 18. Krupp M, Marquardt JU, Sahin U, Galle PR, Castle J, Teufel A. RNA-Seq
1248 Atlas - A reference database for gene expression profiling in normal tissue by next
1249 generation sequencing. *Bioinformatics*. 2012;28. doi: 10.1093/bioinformatics/bts084.
- 1250 19. Oliver S. Proteomics: Guilt-by-association goes global. *Nature*.
1251 2000;403(6770):601-3. doi: doi.org/10.1038/35001165.
- 1252 20. Xiang R, Oddy VH, Archibald AL, Vercoe PE, Dalrymple BP. Epithelial,
1253 metabolic and innate immunity transcriptomic signatures differentiating the rumen
1254 from other sheep and mammalian gastrointestinal tract tissues. *PeerJ*.
1255 2016;4:e1762. doi: 10.7717/peerj.1762.
- 1256 21. Mabbott NA, Kenneth Baillie J, Hume DA, Freeman TC. Meta-analysis of
1257 lineage-specific gene expression signatures in mouse leukocyte populations.
1258 *Immunobiology*. 2010;215. doi: 10.1016/j.imbio.2010.05.012.
- 1259 22. Mabbott NA, Kenneth Baillie J, Kobayashi A, Donaldson DS, Ohmori H, Yoon
1260 SO, et al. Expression of mesenchyme-specific gene signatures by follicular dendritic
1261 cells: insights from the meta-analysis of microarray data from multiple mouse cell
1262 populations. *Immunology*. 2011;133. doi: 10.1111/j.1365-2567.2011.03461.x.
- 1263 23. Clop A, Marcq F, Takeda H, Pirottin D, Tordoir X, Bibe B, et al. A mutation
1264 creating a potential illegitimate microRNA target site in the myostatin gene affects
1265 muscularity in sheep. *Nat Genet*. 2006;38(7):813-8. doi: doi.org/10.1038/ng1810.
- 1266 24. Blackface Sheep Breeders Association [1st March 2017]. Available from:
1267 <http://www.scottish-blackface.co.uk/>.

- 1268 25. Andersson L, Archibald AL, Bottema CD, Brauning R, Burgess SC, Burt DW,
1269 et al. Coordinated international action to accelerate genome-to-phenome with
1270 FAANG, the Functional Annotation of Animal Genomes project. *Genome Biology*.
1271 2015;16(1):57. doi: 10.1186/s13059-015-0622-4.
- 1272 26. Tuggle CK, Giuffra E, White SN, Clarke L, Zhou H, Ross PJ, et al. GO-
1273 FAANG meeting: a Gathering On Functional Annotation of Animal Genomes. *Animal*
1274 *Genetics*. 2016;47(5):528-33. doi: 10.1111/age.12466.
- 1275 27. Carninci P, Kasukawa T, Katayama S, Gough J, Frith MC, Maeda N, et al.
1276 The transcriptional landscape of the mammalian genome. *Science*. 2005;309. doi:
1277 10.1126/science.1112014.
- 1278 28. Bray NL, Pimentel H, Melsted P, Pachter L. Near-optimal probabilistic RNA-
1279 seq quantification. *Nat Biotech*. 2016;34(525–527). doi: doi.org/10.1038/nbt.3519.
- 1280 29. Robert C, Watson M. Errors in RNA-Seq quantification affect genes of
1281 relevance to human disease. *Genome Biology*. 2015;16:177. doi: 10.1186/s13059-
1282 015-0734-x.
- 1283 30. Bush SJ, McCulloch MEB, Summers KM, Hume DA, Clark EL. Integration of
1284 quantitated expression estimates from polyA-selected and rRNA-depleted RNA-seq
1285 libraries. *BMC Bioinformatics*. 2017; *Accepted Pending Minor Revisions*.
- 1286 31. Kumar S, Stecher G, Tamura K. MEGA7: Molecular Evolutionary Genetics
1287 Analysis Version 7.0 for Bigger Datasets. *Molecular Biology and Evolution*.
1288 2016;33(7):1870-4. doi: 10.1093/molbev/msw054.
- 1289 32. Rambaut A. FigTree v1.4.0 2016 [16th March 2017]. v1.4.3:[Available from:
1290 <http://tree.bio.ed.ac.uk/software/figtree/>].
- 1291 33. Guo S, Lim D, Dong Z, Saunders TL, Ma PX, Marcelo CL, et al. Dentin
1292 sialophosphoprotein: a regulatory protein for dental pulp stem cell identity and fate.

- 1293 Stem Cells Dev. 2014;23(23):2883-94. Epub 2014/07/17. doi:
1294 10.1089/scd.2014.0066.
- 1295 34. Wyatt K, Gao C, Tsai JY, Fariss RN, Ray S, Wistow G. A role for lengsin, a
1296 recruited enzyme, in terminal differentiation in the vertebrate lens. J Biol Chem.
1297 2008;283(10):6607-15. Epub 2008/01/08. doi: 10.1074/jbc.M709144200.
- 1298 35. Pruitt KD, Tatusova T, Maglott DR. NCBI Reference Sequence (RefSeq): a
1299 curated non-redundant sequence database of genomes, transcripts and proteins.
1300 Nucleic acids research. 2005;33(Database Issue):D501-D4. doi: 10.1093/nar/gki025.
- 1301 36. Freeman TC, Goldovsky L, Brosch M, van Dongen S, Maziere P, Grocock RJ,
1302 et al. Construction, visualisation, and clustering of transcription networks from
1303 microarray expression data. PLoS computational biology. 2007;3(10):2032-42. Epub
1304 2007/10/31. doi: 10.1371/journal.pcbi.0030206.
- 1305 37. Theocharidis A, van Dongen S, Enright AJ, Freeman TC. Network
1306 visualization and analysis of gene expression data using BioLayout Express(3D).
1307 Nat Protoc. 2009;4(10):1535-50. Epub 2009/10/03. doi: 10.1038/nprot.2009.177.
- 1308 38. Kajeka. Miru 見る 2016 [16th March 2017]. Available from:
1309 <https://kajeka.com/miru/miru-about/>.
- 1310 39. van Dongen S, Abreu-Goodger C. Using MCL to extract clusters from
1311 networks. Methods Mol Biol. 2012;804:281-95. Epub 2011/12/07. doi: 10.1007/978-
1312 1-61779-361-5_15.
- 1313 40. Ashburner M, Ball CA, Blake JA, Botstein D, Butler H, Cherry JM, et al. Gene
1314 ontology: tool for the unification of biology. The Gene Ontology Consortium. Nat
1315 Genet. 2000;25. doi: 10.1038/75556.
- 1316 41. Hume DA, Summers KM, Raza S, Baillie JK, Freeman TC. Functional
1317 clustering and lineage markers: insights into cellular differentiation and gene function

- 1318 from large-scale microarray studies of purified primary cell populations. *Genomics*.
1319 2010;95. doi: 10.1016/j.ygeno.2010.03.002.
- 1320 42. Stumvoll M, Meyer C, Perriello G, Kreider M, Welle S, Gerich J. Human
1321 kidney and liver gluconeogenesis: evidence for organ substrate selectivity. *American*
1322 *Journal of Physiology - Endocrinology And Metabolism*. 1998;274(5):E817.
- 1323 43. Ayyar VS, Almon RR, DuBois DC, Sukumaran S, Qu J, Jusko WJ. Functional
1324 proteomic analysis of corticosteroid pharmacodynamics in rat liver: Relationship to
1325 hepatic stress, signaling, energy regulation, and drug metabolism. *Journal of*
1326 *Proteomics*. doi: doi.org/10.1016/j.jprot.2017.03.007.
- 1327 44. Consortium F. ZENBU: a collaborative, omics data integration and interactive
1328 visualization system 2017 [27th March 2017]. Available from:
1329 <http://fantom.gsc.riken.jp/zenbu/>.
- 1330 45. Severin J, Lizio M, Harshbarger J, Kawaji H, Daub CO, Hayashizaki Y, et al.
1331 Interactive visualization and analysis of large-scale sequencing datasets using
1332 ZENBU. *Nat Biotech*. 2014;32(3):217-9. doi: doi.org/10.1038/nbt.2840.
- 1333 46. Basten SG, Giles RH. Functional aspects of primary cilia in signaling, cell
1334 cycle and tumorigenesis. *Cilia*. 2013;2(1):6. doi: 10.1186/2046-2530-2-6.
- 1335 47. Izawa I, Goto H, Kasahara K, Inagaki M. Current topics of functional links
1336 between primary cilia and cell cycle. *Cilia*. 2015;4(1):12. doi: 10.1186/s13630-015-
1337 0021-1.
- 1338 48. Jackson PK. Do cilia put brakes on the cell cycle? *Nat Cell Biol*. 2011;13. doi:
1339 10.1038/ncb0411-340.
- 1340 49. Doig TN, Hume DA, Theocharidis T, Goodlad JR, Gregory CD, Freeman TC.
1341 Coexpression analysis of large cancer datasets provides insight into the cellular

- 1342 phenotypes of the tumour microenvironment. *BMC Genomics*. 2013;14(1):469. doi:
1343 10.1186/1471-2164-14-469.
- 1344 50. Calvo SE, Clauser KR, Mootha VK. MitoCarta2.0: an updated inventory of
1345 mammalian mitochondrial proteins. *Nucleic Acids Research*. 2016;44(Database
1346 issue):D1251-D7. doi: 10.1093/nar/gkv1003.
- 1347 51. Sharma S, Sud N, Wiseman DA, Carter AL, Kumar S, Hou Y, et al. Altered
1348 carnitine homeostasis is associated with decreased mitochondrial function and
1349 altered nitric oxide signaling in lambs with pulmonary hypertension. *American
1350 Journal of Physiology - Lung Cellular and Molecular Physiology*. 2008;294(1):L46.
1351 doi: 10.1152/ajplung.00247.2007.
- 1352 52. McCommis KS, Finck BN. Mitochondrial pyruvate transport: a historical
1353 perspective and future research directions. *The Biochemical Journal*.
1354 2015;466(3):443-54. doi: 10.1042/BJ20141171.
- 1355 53. Xiang R, McNally J, Rowe S, Jonker A, Pinares-Patino CS, Oddy VH, et al.
1356 Gene network analysis identifies rumen epithelial cell proliferation, differentiation and
1357 metabolic pathways perturbed by diet and correlated with methane production.
1358 *Scientific Reports*. 2016;6:39022. doi: doi.org/10.1038/srep39022.
- 1359 54. Hofmann RR. Evolutionary steps of ecophysiological adaptation and
1360 diversification of ruminants: a comparative view of their digestive system. *Oecologia*.
1361 1989;78(4):443-57. doi: 10.1007/BF00378733.
- 1362 55. Rabbani I, Siegling-Vlitakis C, Noci B, Martens H. Evidence for NHE3-
1363 mediated Na transport in sheep and bovine forestomach. *American Journal of
1364 Physiology - Regulatory, Integrative and Comparative Physiology*.
1365 2011;301(2):R313. doi: 10.1152/ajpregu.00580.2010.

- 1366 56. Foster AM, Baliwag J, Chen CS, Guzman AM, Stoll SW, Gudjonsson JE, et
1367 al. IL-36 Promotes Myeloid Cell Infiltration, Activation, and Inflammatory Activity in
1368 Skin. *The Journal of Immunology*. 2014;192(12):6053. doi:
1369 10.4049/jimmunol.1301481.
- 1370 57. Perkins ND. Integrating cell-signalling pathways with NF- κ B and IKK
1371 function. *Nat Rev Mol Cell Biol*. 2007;8(1):49-62. doi: 10.1038/nrm2083.
- 1372 58. Palmer C, Diehn M, Alizadeh AA, Brown PO. Cell-type specific gene
1373 expression profiles of leukocytes in human peripheral blood. *BMC Genomics*.
1374 2006;7(1):115. doi: 10.1186/1471-2164-7-115.
- 1375 59. Margraf S, Garner LI, Wilson TJ, Brown MH. A polymorphism in a
1376 phosphotyrosine signalling motif of CD229 (Ly9, SLAMF3) alters SH2 domain
1377 binding and T-cell activation. *Immunology*. 2015;146(3):392-400. doi:
1378 10.1111/imm.12513.
- 1379 60. Akira S, Takeda K. Toll-like receptor signalling. *Nat Rev Immunol*.
1380 2004;4(7):499-511. doi: 10.1038/nri1391.
- 1381 61. Baillie JK, Arner E, Daub C, De Hoon M, Itoh M, Kawaji H, et al. Analysis of
1382 the human monocyte-derived macrophage transcriptome and response to
1383 lipopolysaccharide provides new insights into genetic aetiology of inflammatory
1384 bowel disease. *PLoS Genetics*. 2017;13(3):e1006641. doi:
1385 10.1371/journal.pgen.1006641.
- 1386 62. Pflanz S, Timans JC, Cheung J, Rosales R, Kanzler H, Gilbert J, et al. IL-27,
1387 a Heterodimeric Cytokine Composed of EBI3 and p28 Protein, Induces Proliferation
1388 of Naive CD4⁺ T Cells. *Immunity*. 2002;16(6):779-90. doi: doi.org/10.1016/S1074-
1389 7613(02)00324-2.

- 1390 63. Hume DA, Ross IL, Himes SR, Sasmono RT, Wells CA, Ravasi T. The
1391 mononuclear phagocyte system revisited. *Journal of Leukocyte Biology*.
1392 2002;72(4):621-7.
- 1393 64. Moestrup SK, Moller HJ. CD163: a regulated hemoglobin scavenger receptor
1394 with a role in the anti-inflammatory response. *Annals of Medicine*. 2004;36(5):347-
1395 54.
- 1396 65. Bain CC, Mowat AM. Intestinal macrophages – specialised adaptation to a
1397 unique environment. *European Journal of Immunology*. 2011;41(9):2494-8. doi:
1398 10.1002/eji.201141714.
- 1399 66. Vogt L, Schmitz N, Kurrer MO, Bauer M, Hinton HI, Behnke S, et al. VSIG4, a
1400 B7 family–related protein, is a negative regulator of T cell activation. *Journal of*
1401 *Clinical Investigation*. 2006;116(10):2817-26. doi: 10.1172/JCI25673.
- 1402 67. Luo L, Bokil NJ, Wall AA, Kapetanovic R, Lansdaal NM, Marceline F, et al.
1403 SCIMP is a transmembrane non-TIR TLR adaptor that promotes proinflammatory
1404 cytokine production from macrophages. *Nature Communications*. 2017;8:14133. doi:
1405 10.1038/ncomms14133.
- 1406 68. Bonifer C, Hume DA. The transcriptional regulation of the Colony-Stimulating
1407 Factor 1 Receptor (*csf1r*) gene during hematopoiesis *Frontiers in Bioscience*.
1408 2008;(13):549-60.
- 1409 69. Hume DA, Yue X, Ross IL, Favot P, Lichanska A, Ostrowski MC. Regulation
1410 of CSF-1 receptor expression. *Molecular Reproduction and Development*.
1411 1997;46(1):46-53. doi: 10.1002/(SICI)1098-2795(199701)46:1<46::AID-
1412 MRD8>3.0.CO;2-R.

- 1413 70. Uhlén M, Fagerberg L, Hallström BM, Lindskog C, Oksvold P, Mardinoglu A,
1414 et al. Tissue-based map of the human proteome. *Science*. 2015;347(6220). doi:
1415 10.1126/science.1260419.
- 1416 71. Wu C, Jin X, Tsueng G, Afrasiabi C, Su AI. BioGPS: building your own mash-
1417 up of gene annotations and expression profiles. *Nucleic Acids Research*.
1418 2016;44(D1):D313-D6. doi: 10.1093/nar/gkv1104.
- 1419 72. Djureinovic D, Fagerberg L, Hallström B, Danielsson A, Lindskog C, Uhlén M,
1420 et al. The human testis-specific proteome defined by transcriptomics and antibody-
1421 based profiling. *MHR: Basic science of reproductive medicine*. 2014;20(6):476-88.
1422 doi: 10.1093/molehr/gau018.
- 1423 73. Yu NY-L, Hallström BM, Fagerberg L, Ponten F, Kawaji H, Carninci P, et al.
1424 Complementing tissue characterization by integrating transcriptome profiling from
1425 the Human Protein Atlas and from the FANTOM5 consortium. *Nucleic Acids*
1426 *Research*. 2015;43(14):6787-98. doi: 10.1093/nar/gkv608.
- 1427 74. Baillet A, Le Bouffant R, Volff JN, Luangpraseuth A, Pomerol E, Thépot D, et
1428 al. TOPAZ1, a Novel Germ Cell-Specific Expressed Gene Conserved during
1429 Evolution across Vertebrates. *PLoS ONE*. 2011;6(11):e26950. doi:
1430 10.1371/journal.pone.0026950.
- 1431 75. Olesen C, Larsen NJ, Byskov AG, Harboe TL, Tommerup N. Human FATE is
1432 a novel X-linked gene expressed in fetal and adult testis. *Molecular and Cellular*
1433 *Endocrinology*. 2001;184(1–2):25-32. doi: doi.org/10.1016/S0303-7207(01)00666-9.
- 1434 76. Osaki E, Nishina Y, Inazawa J, Copeland NG, Gilbert DJ, Jenkins NA, et al.
1435 Identification of a novel Sry-related gene and its germ cell-specific expression.
1436 *Nucleic Acids Research*. 1999;27(12):2503-10.

- 1437 77. Calloni R, Cordero EAA, Henriques JAP, Bonatto D. Reviewing and Updating
1438 the Major Molecular Markers for Stem Cells. *Stem Cells and Development*.
1439 2013;22(9):1455-76. doi: 10.1089/scd.2012.0637.
- 1440 78. Kehler J, Tolkunova E, Koschorz B, Pesce M, Gentile L, Boiani M, et al. Oct4
1441 is required for primordial germ cell survival. *EMBO reports*. 2004;5(11):1078-83. doi:
1442 10.1038/sj.embor.7400279.
- 1443 79. Juengel JL, Bodensteiner KJ, Heath DA, Hudson NL, Moeller CL, Smith P, et
1444 al. Physiology of GDF9 and BMP15 signalling molecules. *Animal Reproduction
1445 Science*. 2004;82–83:447-60. doi: doi.org/10.1016/j.anireprosci.2004.04.021.
- 1446 80. McNatty KP, Juengel JL, Wilson T, Galloway SM, Davis GH. Genetic
1447 mutations influencing ovulation rate in sheep. *Reproduction, Fertility and
1448 Development*. 2002;13(8):549-55. doi: doi.org/10.1071/RD01078.
- 1449 81. Palomera CL, Morales RAA. Genes with major effect on fertility in sheep.
1450 *Revista Mexicana de Ciencias Pecuarias*. 2014;5(1):107-30.
- 1451 82. Imahara SD, Jelacic S, Junker CE, O'Keefe GE. The influence of gender on
1452 human innate immunity. *Surgery*. 2005;138(2):275-82. doi:
1453 doi.org/10.1016/j.surg.2005.03.020.
- 1454 83. Marriott I, Huet-Hudson YM. Sexual dimorphism in innate immune responses
1455 to infectious organisms. *Immunologic Research*. 2006;34(3):177-92. doi:
1456 10.1385/IR:34:3:177.
- 1457 84. Everhardt Queen A, Moerdyk-Schauwecker M, McKee LM, Leamy LJ, Huet
1458 YM. Differential Expression of Inflammatory Cytokines and Stress Genes in Male
1459 and Female Mice in Response to a Lipopolysaccharide Challenge. *PLoS ONE*.
1460 2016;11(4):e0152289. doi: 10.1371/journal.pone.0152289.

- 1461 85. Lamason R, Zhao P, Rawat R, Davis A, Hall JC, Chae JJ, et al. Sexual
1462 dimorphism in immune response genes as a function of puberty. *BMC Immunology*.
1463 2006;7(1):2. doi: 10.1186/1471-2172-7-2.
- 1464 86. Forde N, Maillo V, O'Gaora P, Simintiras CA, Sturmey RG, Ealy AD, et al.
1465 Sexually Dimorphic Gene Expression in Bovine Conceptuses at the Initiation of
1466 Implantation. *Biology of Reproduction*. 2016;95(4):92 1-8. doi:
1467 10.1095/biolreprod.116.139857.
- 1468 87. Bermejo-Alvarez P, Rizos D, Rath D, Lonergan P, Gutierrez-Adan A. Sex
1469 determines the expression level of one third of the actively expressed genes in
1470 bovine blastocysts. *Proc Natl Acad Sci USA*. 2010;107. doi:
1471 10.1073/pnas.0913843107.
- 1472 88. Mentzel CMJ, Anthon C, Jacobsen MJ, Karlskov-Mortensen P, Bruun CS,
1473 Jørgensen CB, et al. Gender and Obesity Specific MicroRNA Expression in Adipose
1474 Tissue from Lean and Obese Pigs. *PLoS ONE*. 2015;10(7):e0131650. doi:
1475 10.1371/journal.pone.0131650.
- 1476 89. Zhang J, Zhou C, Ma J, Chen L, Jiang A, Zhu L, et al. Breed, sex and
1477 anatomical location-specific gene expression profiling of the porcine skeletal
1478 muscles. *BMC Genetics*. 2013;14(1):53. doi: 10.1186/1471-2156-14-53.
- 1479 90. Wood Shona H, Christian Helen C, Miedzinska K, Saer Ben RC, Johnson M,
1480 Paton B, et al. Binary Switching of Calendar Cells in the Pituitary Defines the Phase
1481 of the Circannual Cycle in Mammals. *Current Biology*. 2015;25(20):2651-62. doi:
1482 doi.org/10.1016/j.cub.2015.09.014.
- 1483 91. Bjelobaba I, Janjic MM, Kucka M, Stojilkovic SS. Cell Type-Specific Sexual
1484 Dimorphism in Rat Pituitary Gene Expression During Maturation. *Biology of*
1485 *Reproduction*. 2015;93(1):21. doi: 10.1095/biolreprod.115.129320.

- 1486 92. Oidovsambuu O, Nyamsuren G, Liu S, Göring W, Engel W, Adham IM.
1487 Adhesion Protein VSIG1 Is Required for the Proper Differentiation of Glandular
1488 Gastric Epithelia. PLoS ONE. 2011;6(10):e25908. doi:
1489 10.1371/journal.pone.0025908.
- 1490 93. Ellegren H, Parsch J. The evolution of sex-biased genes and sex-biased gene
1491 expression. Nat Rev Genet. 2007;8(9):689-98. doi: 10.1038/nrg2167.
- 1492 94. Gillespie JR, Flanders F. Modern Livestock & Poultry Production. 8th Edition
1493 ed: Delmar; 2009.
- 1494 95. Zonabend König E, Ojango JMK, Audho J, Mirkena T, Strandberg E, Okeyo
1495 AM, et al. Live weight, conformation, carcass traits and economic values of ram
1496 lambs of Red Maasai and Dorper sheep and their crosses. Tropical Animal Health
1497 and Production. 2017;49(1):121-9. doi: 10.1007/s11250-016-1168-5.
- 1498 96. Zonabend König E, Strandberg E, Ojango JMK, Mirkena T, Okeyo AM,
1499 Philipsson J. Purebreeding of Red Maasai and crossbreeding with Dorper sheep in
1500 different environments in Kenya. Journal of Animal Breeding and Genetics.
1501 2017:n/a-n/a. doi: 10.1111/jbg.12260.
- 1502 97. Rashid MM, Runci A, Polletta L, Carnevale I, Morgante E, Foglio E, et al.
1503 Muscle LIM protein/CSRP3: a mechanosensor with a role in autophagy. Cell Death
1504 Discovery. 2015;1:15014. doi: doi.org/10.1038/cddiscovery.2015.14.
- 1505 98. Jan AT, Lee EJ, Choi I. Fibromodulin: A regulatory molecule maintaining
1506 cellular architecture for normal cellular function. Int J Biochem Cell Biol. 2016;80:66-
1507 70. Epub 2016/10/04. doi: 10.1016/j.biocel.2016.09.023.
- 1508 99. Funderburgh JL, Mann MM, Funderburgh ML. Keratocyte Phenotype
1509 Mediates Proteoglycan Structure: A Role for Fibroblasts in Corneal Fibrosis. The

- 1510 Journal of Biological Chemistry. 2003;278(46):45629-37. doi:
1511 10.1074/jbc.M303292200.
- 1512 100. Hadler-Olsen E, Solli AI, Hafstad A, Winberg JO, Uhlin-Hansen L. Intracellular
1513 MMP-2 activity in skeletal muscle is associated with type II fibers. J Cell Physiol.
1514 2015;230(1):160-9. Epub 2014/06/07. doi: 10.1002/jcp.24694.
- 1515 101. Beard NA, Laver DR, Dulhunty AF. Calsequestrin and the calcium release
1516 channel of skeletal and cardiac muscle. Prog Biophys Mol Biol. 2004;85(1):33-69.
1517 Epub 2004/03/31. doi: 10.1016/j.pbiomolbio.2003.07.001.
- 1518 102. Tellam RL, Cockett NE, Vuocolo T, Bidwell CA. Genes Contributing to
1519 Genetic Variation of Muscling in Sheep. Frontiers in Genetics. 2012;3:164. doi:
1520 10.3389/fgene.2012.00164.
- 1521 103. Miar Y, Salehi A, Kolbehdari D, Aleyasin SA. Application of myostatin in
1522 sheep breeding programs: A review. Molecular Biology Research Communications.
1523 2014;3(1):33-43.
- 1524 104. Cassar-Malek I, Passelaigue F, Bernard C, Léger J, Hocquette J-F. Target
1525 genes of myostatin loss-of-function in muscles of late bovine fetuses. BMC
1526 Genomics. 2007;8:63. doi: 10.1186/1471-2164-8-63.
- 1527 105. Wang M, Yu H, Kim YS, Bidwell CA, Kuang S. Myostatin facilitates slow and
1528 inhibits fast myosin heavy chain expression during myogenic differentiation.
1529 Biochemical and Biophysical Research Communications. 2012;426(1):83-8. doi:
1530 doi.org/10.1016/j.bbrc.2012.08.040.
- 1531 106. Allen DL, Loh AS. Posttranscriptional mechanisms involving microRNA-27a
1532 and b contribute to fast-specific and glucocorticoid-mediated myostatin expression in
1533 skeletal muscle. American Journal of Physiology - Cell Physiology.
1534 2011;300(1):C124-C37. doi: 10.1152/ajpcell.00142.2010.

- 1535 107. Mosca B, Eckhardt J, Bergamelli L, Treves S, Bongianino R, De Negri M, et
1536 al. Role of the JP45-Calsequestrin Complex on Calcium Entry in Slow Twitch
1537 Skeletal Muscles. *Journal of Biological Chemistry*. 2016;291(28):14555-65. doi:
1538 10.1074/jbc.M115.709071.
- 1539 108. Moran CM, Garriock RJ, Miller MK, Heimark RL, Mudry RE, Gregorio CC, et
1540 al. Expression of the fast twitch troponin complex, fTnT, fTnI and fTnC, in vascular
1541 smooth muscle. *Cell motility and the cytoskeleton*. 2008;65(8):652-61. doi:
1542 10.1002/cm.20291.
- 1543 109. Odermatt A, Becker S, Khanna VK, Kurzydowski K, Leisner E, Pette D, et al.
1544 Sarcolipin Regulates the Activity of SERCA1, the Fast-twitch Skeletal Muscle
1545 Sarcoplasmic Reticulum Ca²⁺-ATPase. *Journal of Biological Chemistry*.
1546 1998;273(20):12360-9. doi: 10.1074/jbc.273.20.12360.
- 1547 110. Joo ST, Kim GD, Hwang YH, Ryu YC. Control of fresh meat quality through
1548 manipulation of muscle fiber characteristics. *Meat Science*. 2013;95(4):828-36. doi:
1549 doi.org/10.1016/j.meatsci.2013.04.044.
- 1550 111. Goel M, Sienkiewicz AE, Picciani R, Wang J, Lee RK, Bhattacharya SK.
1551 Cochlin, Intraocular Pressure Regulation and Mechanosensing. *PLoS ONE*.
1552 2012;7(4):e34309. doi: 10.1371/journal.pone.0034309.
- 1553 112. Seidenbecher CI, Smalla KH, Fischer N, Gundelfinger ED, Kreutz MR.
1554 Brevican isoforms associate with neural membranes. *J Neurochem*. 2002;83(3):738-
1555 46. Epub 2002/10/23.
- 1556 113. Yamaguchi Y. Brevican: a major proteoglycan in adult brain. *Perspect Dev*
1557 *Neurobiol*. 1996;3(4):307-17. Epub 1996/01/01.
- 1558 114. Holz A, Schwab ME. Developmental expression of the myelin gene MOBP in
1559 the rat nervous system. *J Neurocytol*. 1997;26(7):467-77. Epub 1997/07/01.

- 1560 115. Yoshikawa F, Sato Y, Tohyama K, Akagi T, Hashikawa T, Nagakura-Takagi
1561 Y, et al. Opalin, a Transmembrane Sialylglycoprotein Located in the Central Nervous
1562 System Myelin Paranodal Loop Membrane. *The Journal of Biological Chemistry*.
1563 2008;283(30):20830-40. doi: 10.1074/jbc.M801314200.
- 1564 116. Boggs JM. Myelin basic protein: a multifunctional protein. *Cellular and*
1565 *Molecular Life Sciences*. 2006;63(17):1945-61. doi: 10.1007/s00018-006-6094-7.
- 1566 117. Dwyer CM, Lawrence AB, Brown HE, Simm G. Effect of ewe and lamb
1567 genotype on gestation length, lambing ease and neonatal behaviour of lambs.
1568 *Reprod Fertil Dev* 1996;8(8):1123-9.
- 1569 118. McCloskey E, McAdam JH. Grazing patterns and habitat selection of the
1570 Scottish Blackface compared with a crossbred, using GPS Satellite telemetry collars.
1571 *Advances in Animal Biosciences*. 2010;1(1):171. doi: 10.1017/S2040470010003146.
- 1572 119. Wu C, MacLeod I, Su AI. BioGPS and MyGene.info: organizing online, gene-
1573 centric information. *Nucleic Acids Research*. 2013;41(D1):D561-D5. doi:
1574 10.1093/nar/gks1114.
- 1575 120. Wu C, Orozco C, Boyer J, Leglise M, Goodale J, Batalov S, et al. BioGPS: an
1576 extensible and customizable portal for querying and organizing gene annotation
1577 resources. *Genome Biology*. 2009;10(11):R130. doi: 10.1186/gb-2009-10-11-r130.
- 1578 121. Kim D, Langmead B, Salzberg SL. HISAT: a fast spliced aligner with low
1579 memory requirements. *Nat Meth*. 2015;12(4):357-60. doi:
1580 doi.org/10.1038/nmeth.3317.
- 1581 122. Pertea M, Pertea GM, Antonescu CM, Chang T-C, Mendell JT, Salzberg SL.
1582 StringTie enables improved reconstruction of a transcriptome from RNA-seq reads.
1583 *Nat Biotech*. 2015;33(3):290-5. doi: doi.org/10.1038/nbt.3122.

- 1584 123. Miao X, Luo Q, Qin X. Genome-wide analysis reveals the differential
1585 regulations of mRNAs and miRNAs in Dorset and Small Tail Han sheep muscles.
1586 *Gene*. 2015;562(2):188-96. doi: doi.org/10.1016/j.gene.2015.02.070.
- 1587 124. Suárez-Vega A, Gutiérrez-Gil B, Klopp C, Tosser-Klopp G, Arranz JJ. Variant
1588 discovery in the sheep milk transcriptome using RNA sequencing. *BMC Genomics*.
1589 2017;18(1):170. doi: 10.1186/s12864-017-3581-1.
- 1590 125. Sun L, Bai M, Xiang L, Zhang G, Ma W, Jiang H. Comparative transcriptome
1591 profiling of longissimus muscle tissues from Qianhua Mutton Merino and Small Tail
1592 Han sheep. *Scientific Reports*. 2016;6:33586. doi: doi.org/10.1038/srep33586.
- 1593 126. Peñagaricano F, Valente BD, Steibel JP, Bates RO, Ernst CW, Khatib H, et
1594 al. Searching for causal networks involving latent variables in complex traits:
1595 Application to growth, carcass, and meat quality traits in pigs. *Journal of Animal*
1596 *Science*. 2015;93(10):4617-23. doi: 10.2527/jas.2015-9213.
- 1597 127. Van Laere A-S, Nguyen M, Braunschweig M, Nezer C, Collette C, Moreau L,
1598 et al. A regulatory mutation in IGF2 causes a major QTL effect on muscle growth in
1599 the pig. *Nature*. 2003;425(6960):832-6. doi: doi.org/10.1038/nature02064.
- 1600 128. Banos G, Bramis G, Bush SJ, Clark EL, McCulloch MEB, Smith J, et al. The
1601 genomic architecture of mastitis resistance in dairy sheep. 2017;Under Review.
- 1602 129. Suárez-Vega A, Gutiérrez-Gil B, Klopp C, Tosser-Klopp G, Arranz J-J.
1603 Comprehensive RNA-Seq profiling to evaluate lactating sheep mammary gland
1604 transcriptome. *Scientific Data*. 2016;3:160051. doi: doi.org/10.1038/sdata.2016.51.
- 1605 130. Kapetanovic R, Fairbairn L, Beraldi D, Sester DP, Archibald AL, Tuggle CK, et
1606 al. Pig bone marrow-derived macrophages resemble human macrophages in their
1607 response to bacterial lipopolysaccharide. *J Immunol*. 2012;188. doi:
1608 10.4049/jimmunol.1102649.

- 1609 131. Fairbairn L, Kapetanovic R, Beraldi D, Sester DP, Tuggle CK, Archibald AL, et
1610 al. Comparative Analysis of Monocyte Subsets in the Pig. *The Journal of*
1611 *Immunology*. 2013;190(12):6389-96. doi: 10.4049/jimmunol.1300365.
- 1612 132. Montgomery GW, Sise JA. Extraction of DNA from sheep white blood cells.
1613 *New Zealand Journal of Agricultural Research*. 1990;33(3):437-41. doi:
1614 10.1080/00288233.1990.10428440.
- 1615 133. Pervouchine DD, Djebali S, Breschi A, Davis CA, Barja PP, Dobin A, et al.
1616 Enhanced transcriptome maps from multiple mouse tissues reveal evolutionary
1617 constraint in gene expression. *Nat Commun*. 2015;6. doi: 10.1038/ncomms6903.
- 1618 134. Chitwood J, Rincon G, Kaiser G, Medrano J, Ross P. RNA-seq analysis of
1619 single bovine blastocysts. *BMC Genomics*. 2013;14(1):350. doi: 10.1186/1471-2164-
1620 14-350.
- 1621 135. Martherus RS, Sluiter W, Timmer ED, VanHerle SJ, Smeets HJ, Ayoubi TA.
1622 Functional annotation of heart enriched mitochondrial genes GBAS and CHCHD10
1623 through guilt by association. *Biochem Biophys Res Commun*. 2010;402. doi:
1624 10.1016/j.bbrc.2010.09.109.
- 1625 136. Alexa A, Rahnenfuhrer J. topGO: Enrichment analysis for Gene Ontology
1626 2010. Available from:
1627 <http://www.bioconductor.org/packages/release/bioc/html/topGO.html>.
- 1628 137. Fagerberg L, Hallström BM, Oksvold P, Kampf C, Djureinovic D, Odeberg J,
1629 et al. Analysis of the Human Tissue-specific Expression by Genome-wide Integration
1630 of Transcriptomics and Antibody-based Proteomics. *Molecular & Cellular*
1631 *Proteomics*. 2014;13(2):397-406. doi: 10.1074/mcp.M113.035600.

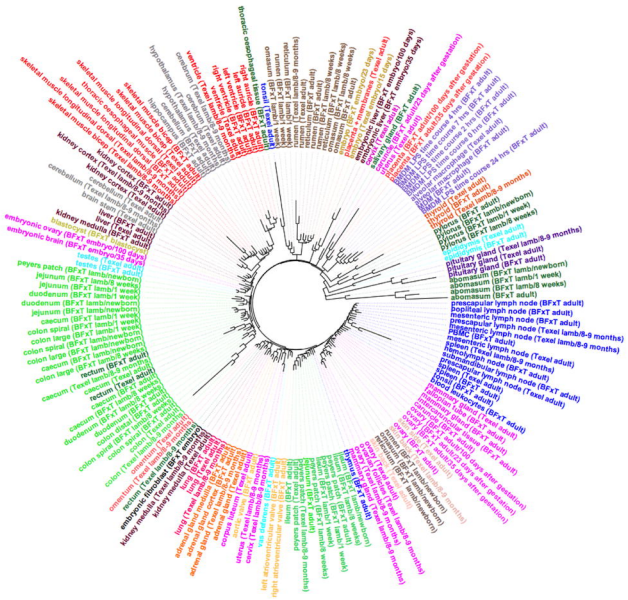
1632 138. Lein ES, Hawrylycz MJ, Ao N, Ayres M, Bensinger A, Bernard A, et al.
1633 Genome-wide atlas of gene expression in the adult mouse brain. *Nature*.
1634 2007;445(7124):168-76. doi: doi.org/10.1038/nature05453.

1635 139. Siddiqui AS, Khattra J, Delaney AD, Zhao Y, Astell C, Asano J, et al. A mouse
1636 atlas of gene expression: Large-scale digital gene-expression profiles from precisely
1637 defined developing C57BL/6J mouse tissues and cells. *Proc Natl Acad Sci USA*.
1638 2005;102(51):18485-90. doi: 10.1073/pnas.0509455102.

1639

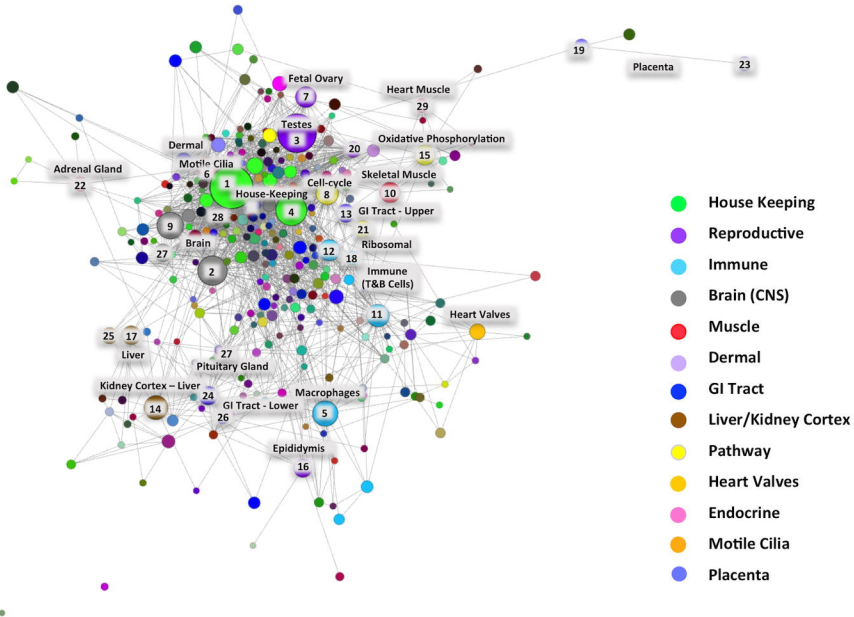
1640

1641

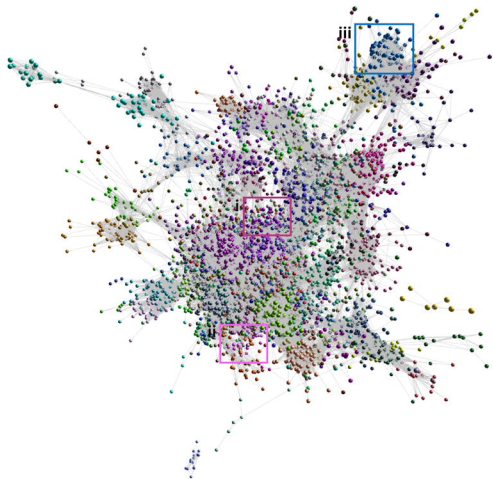


- Male Reproductive
- Female Reproductive
- Immune
- GI Tract (Small/Large Intestine)
- GI Tract (Ileum/Peyer's Patch)
- GI Tract (Rumen Complex)
- GI tract (Other)
- Endocrine
- Kidney/Liver
- Brain
- Skeletal Muscle/Heart
- Heart Valves
- Skin
- Omentum
- Embryo/Blastocysts
- Pituitary Gland
- Embryonic Fibroblasts
- Macrophages
- Placenta
- Lung

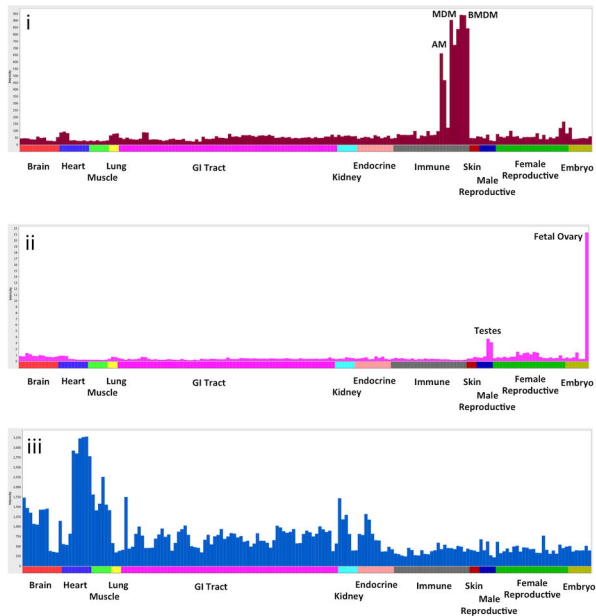




A



B



A



Sire - Texel



Dam – Scottish Blackface

F₁ – Scottish Blackface x Texel

B

